UC SANTA BARBARA

U.S. DEPARTMENT OF ENERGY

Office of Science

Higgs boson width and off-shell contributions to ZZ production

(from Nature Phys. 18 11 (2022) and related analyses)

Ulascan Sarica
on behalf of
the CMS Collaboration

Fermilab Wine & Cheese Seminar
Feb. 3, 2023

Why measure the Higgs boson width?

Are there subdominant contributions to our current production and decay calculations we have not yet included?

Does the Higgs boson interact with particles we cannot detect (e.g. neutrinos)?

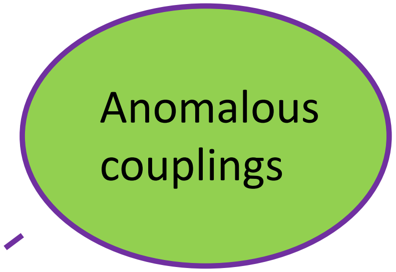

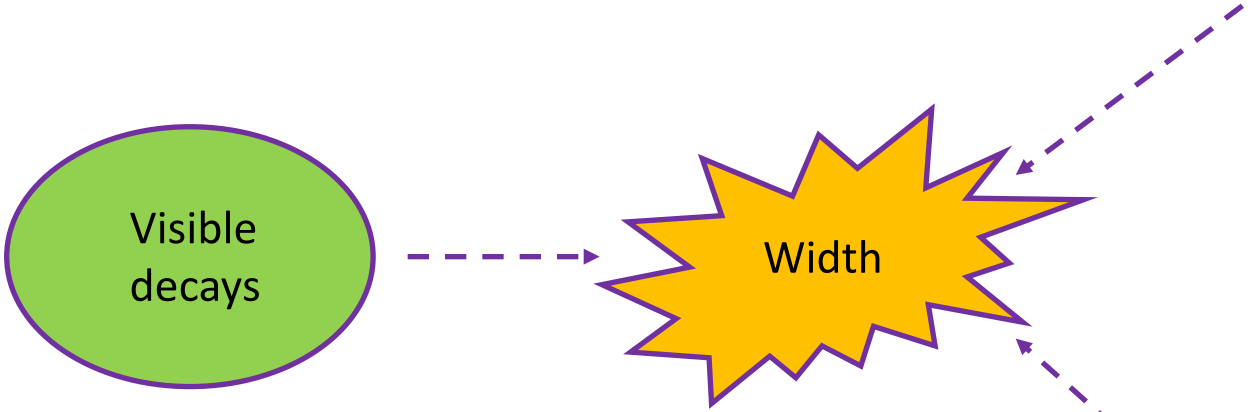

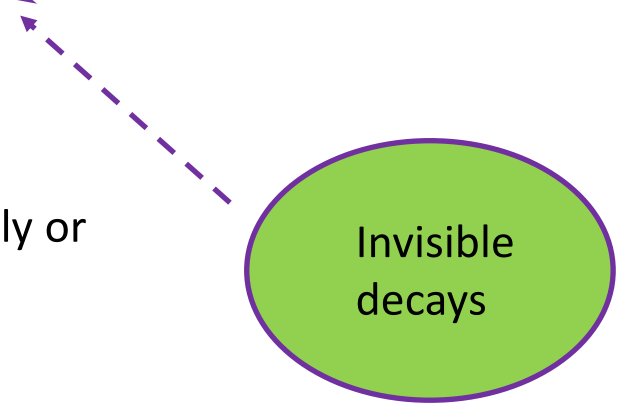

Does it interact with a new type of matter either directly or through loops?

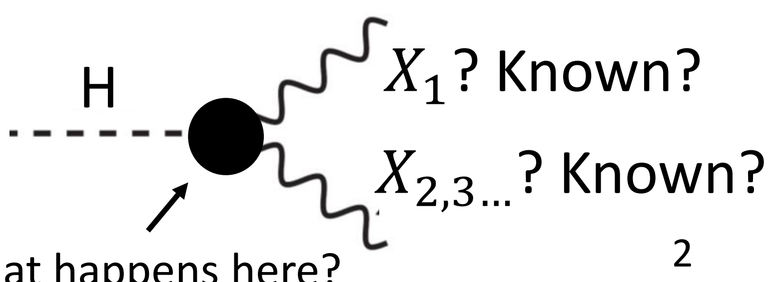

What can we measure?

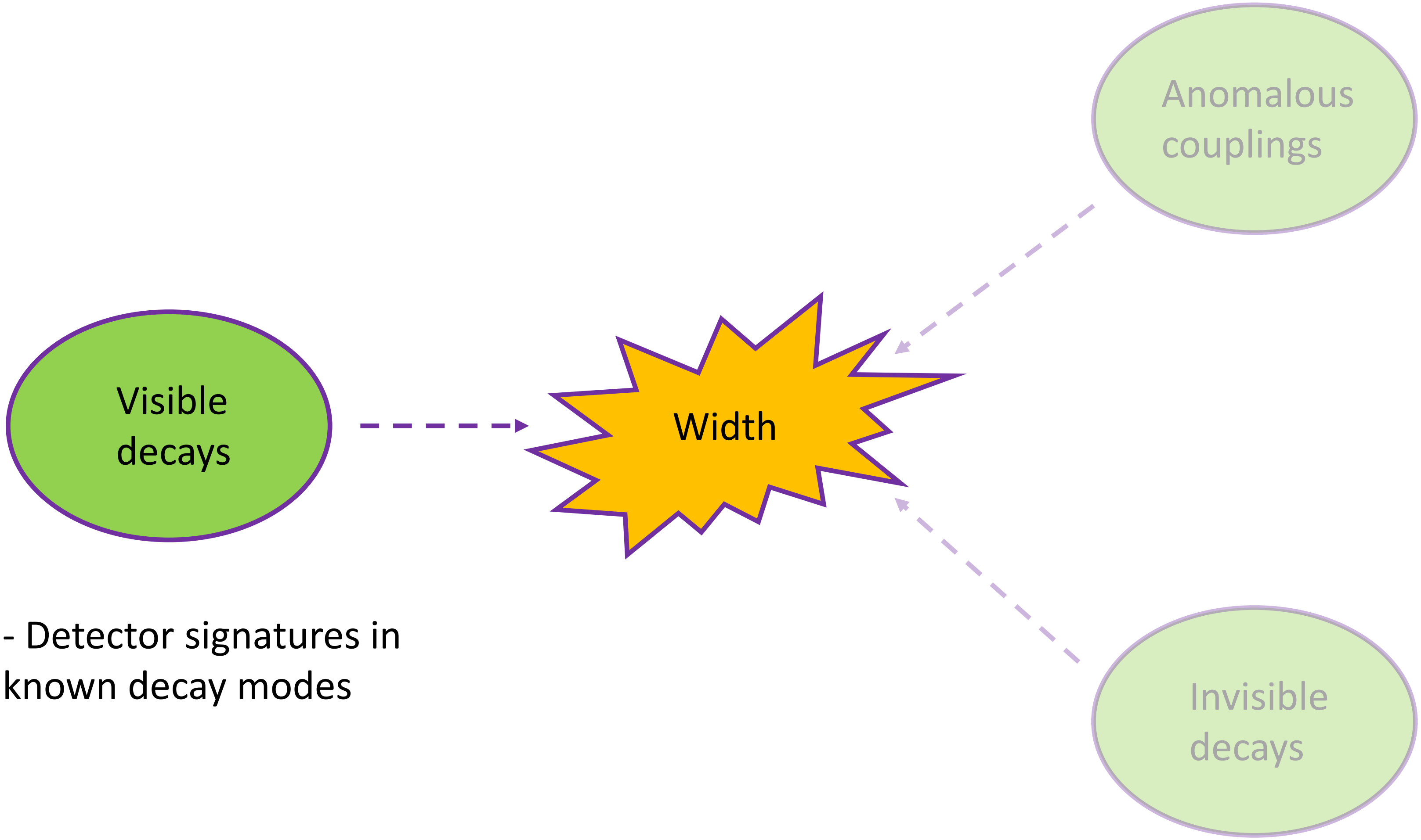

- Detector signatures in known decay modes

What can we measure?

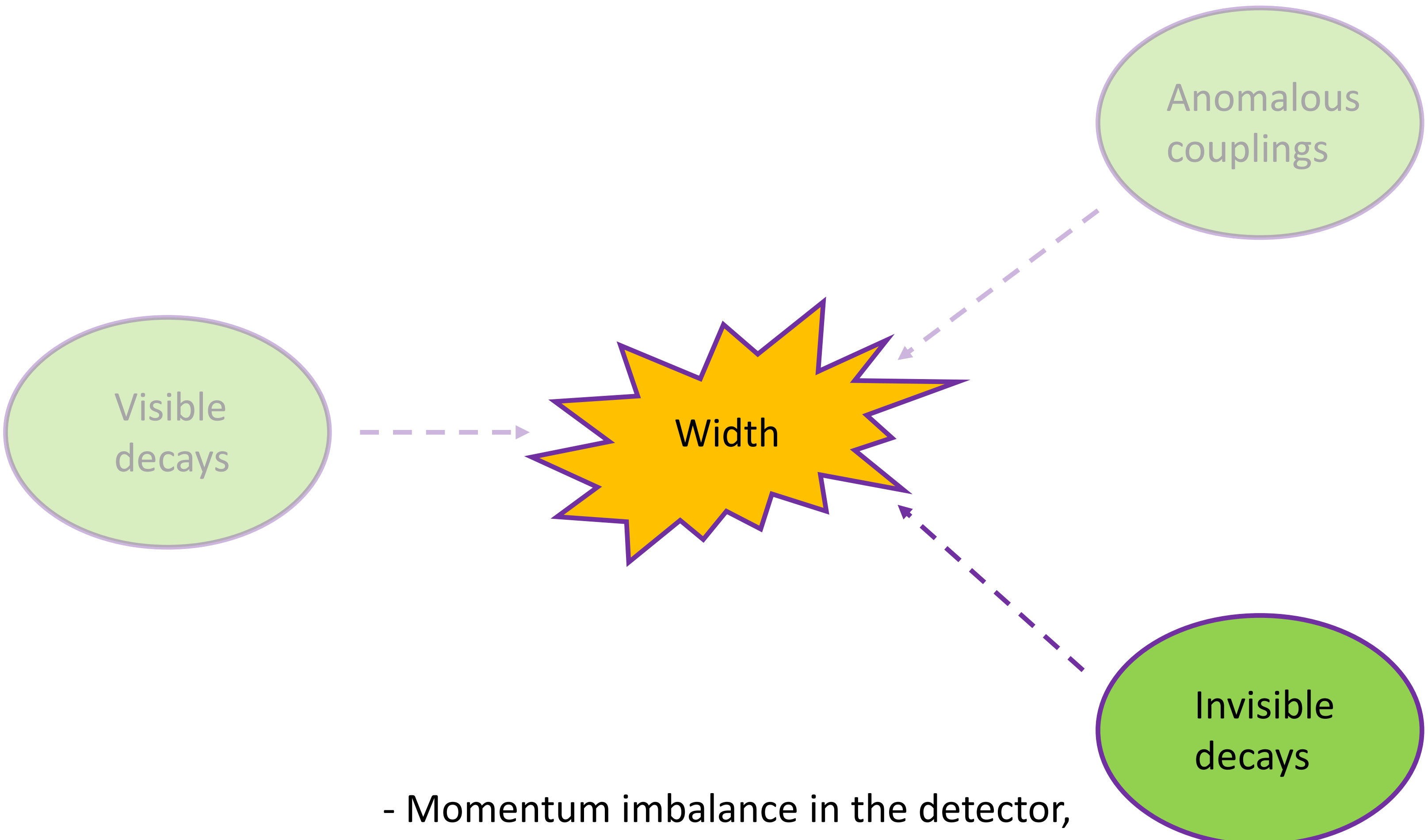

- Momentum imbalance in the detector, excess events wrt. known backgrounds

What can we measure?

- Angular and mass observables
- Production and decay correlations

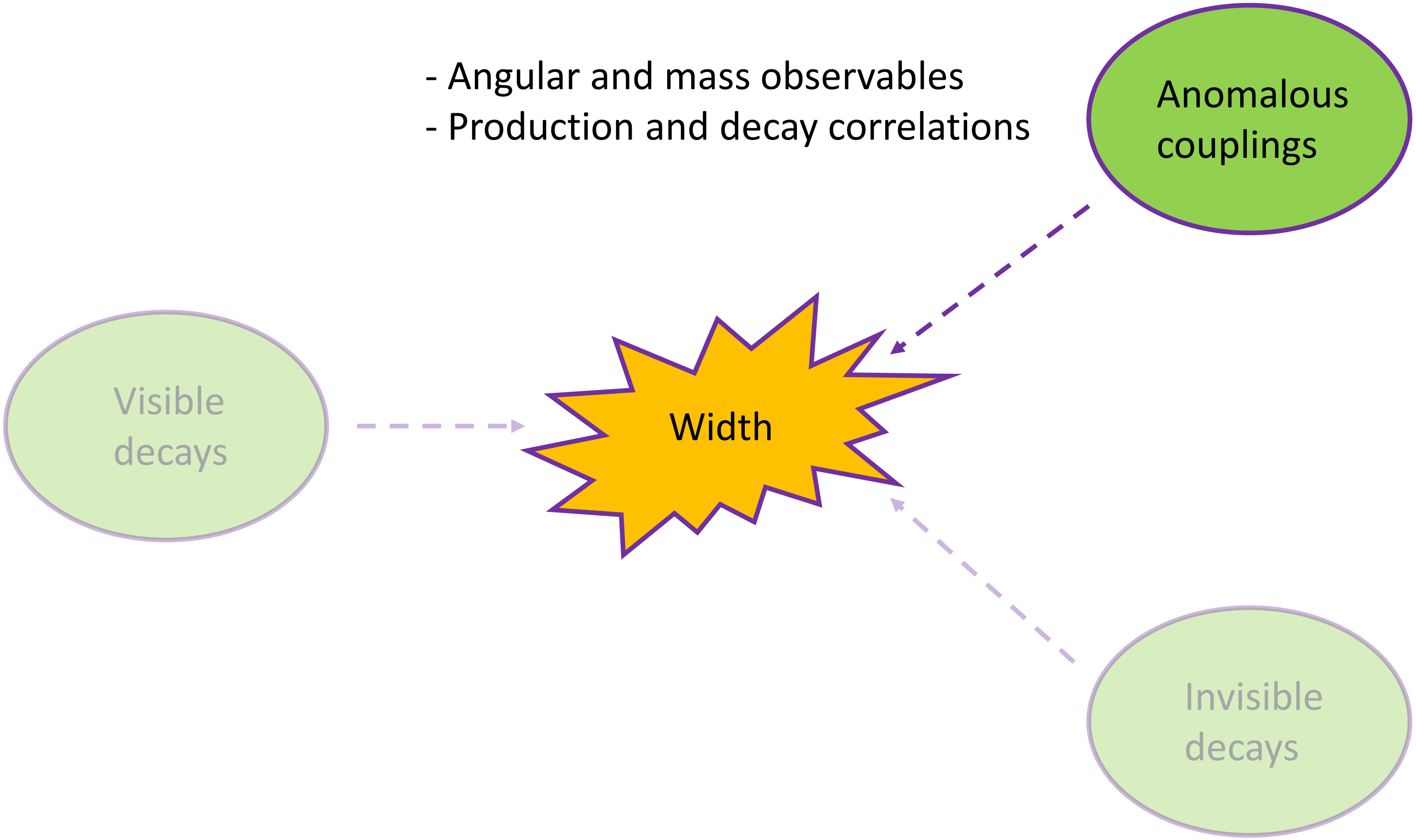

What can we measure?

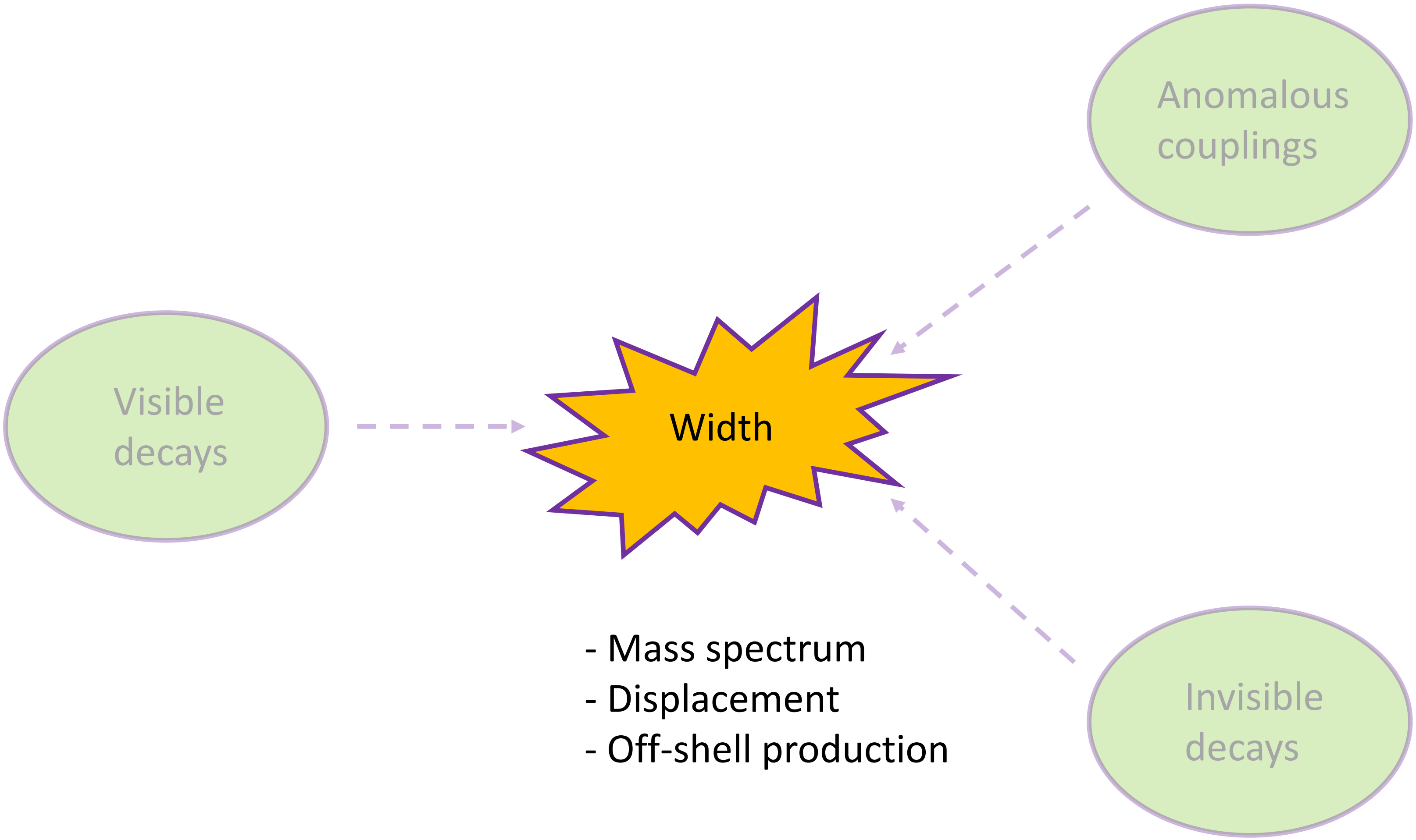

- Mass spectrum
- Displacement
- Off-shell production

What can we measure?

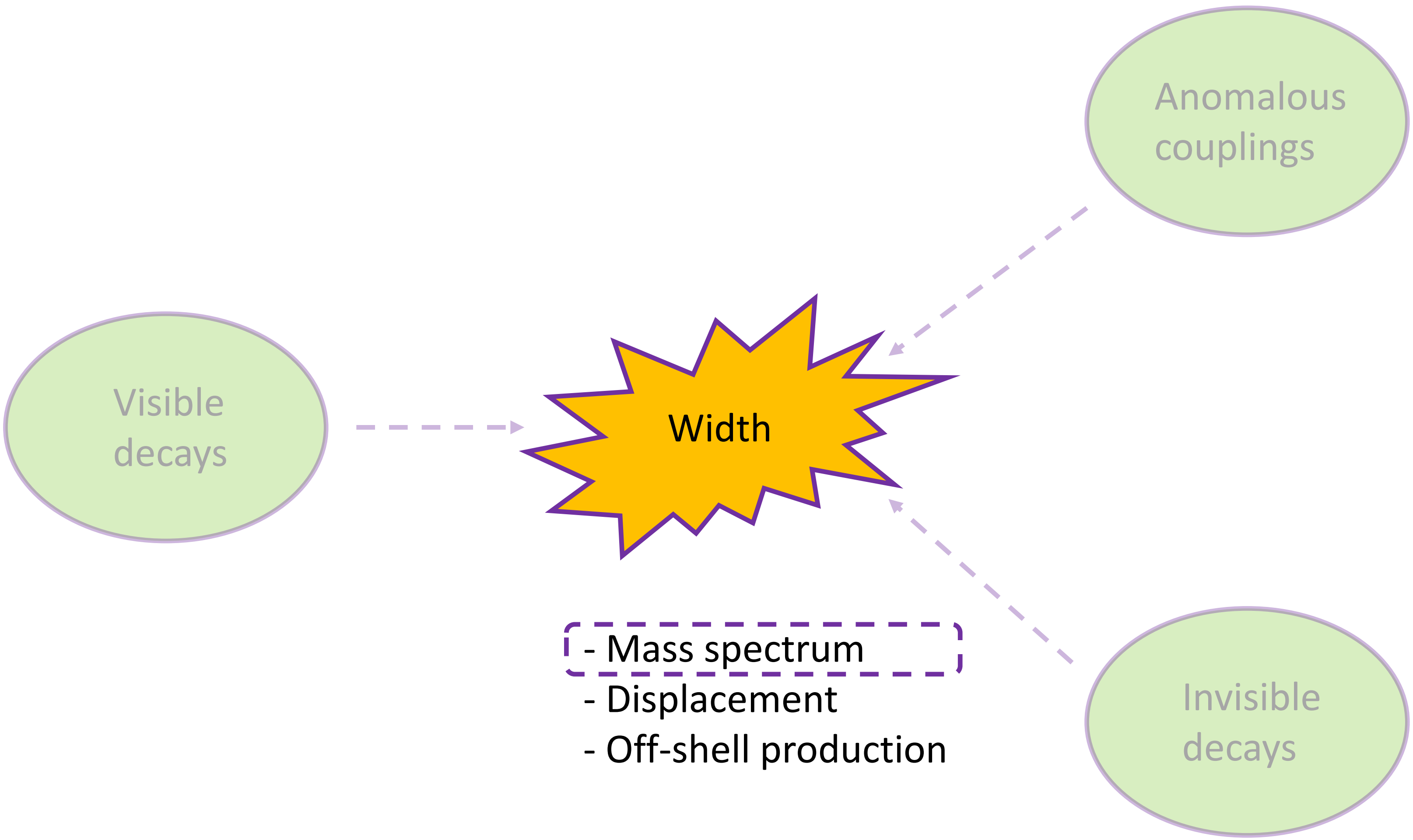

- Mass spectrum
- Displacement
- Off-shell production

SM: 4.1 MeV
Detector resolution: 1 GeV

What can we measure?

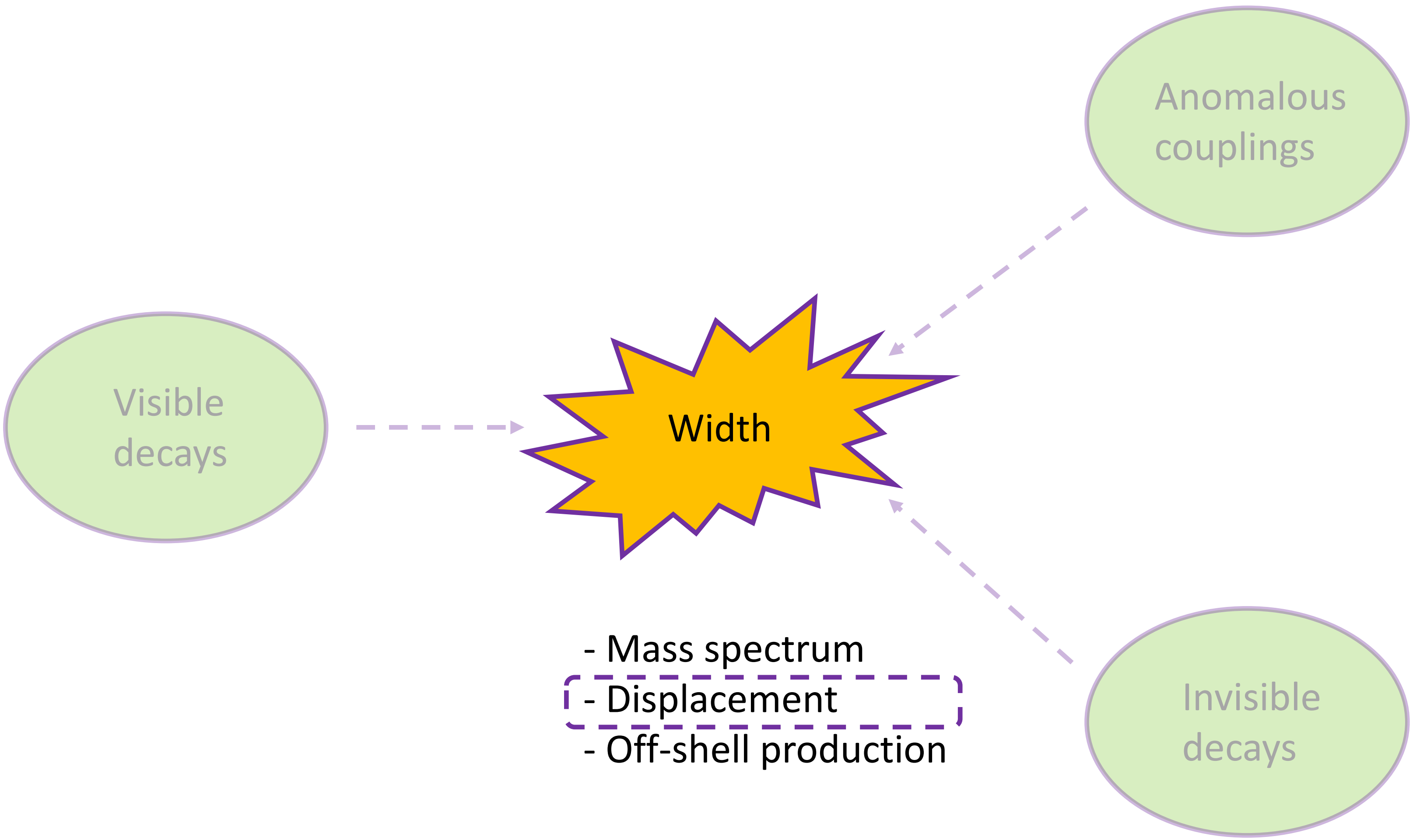

- Mass spectrum
- Displacement
- Off-shell production

SM: 1.6×10^{-22} s
Detector resolution: 1.9×10^{-13} s

What can we measure?

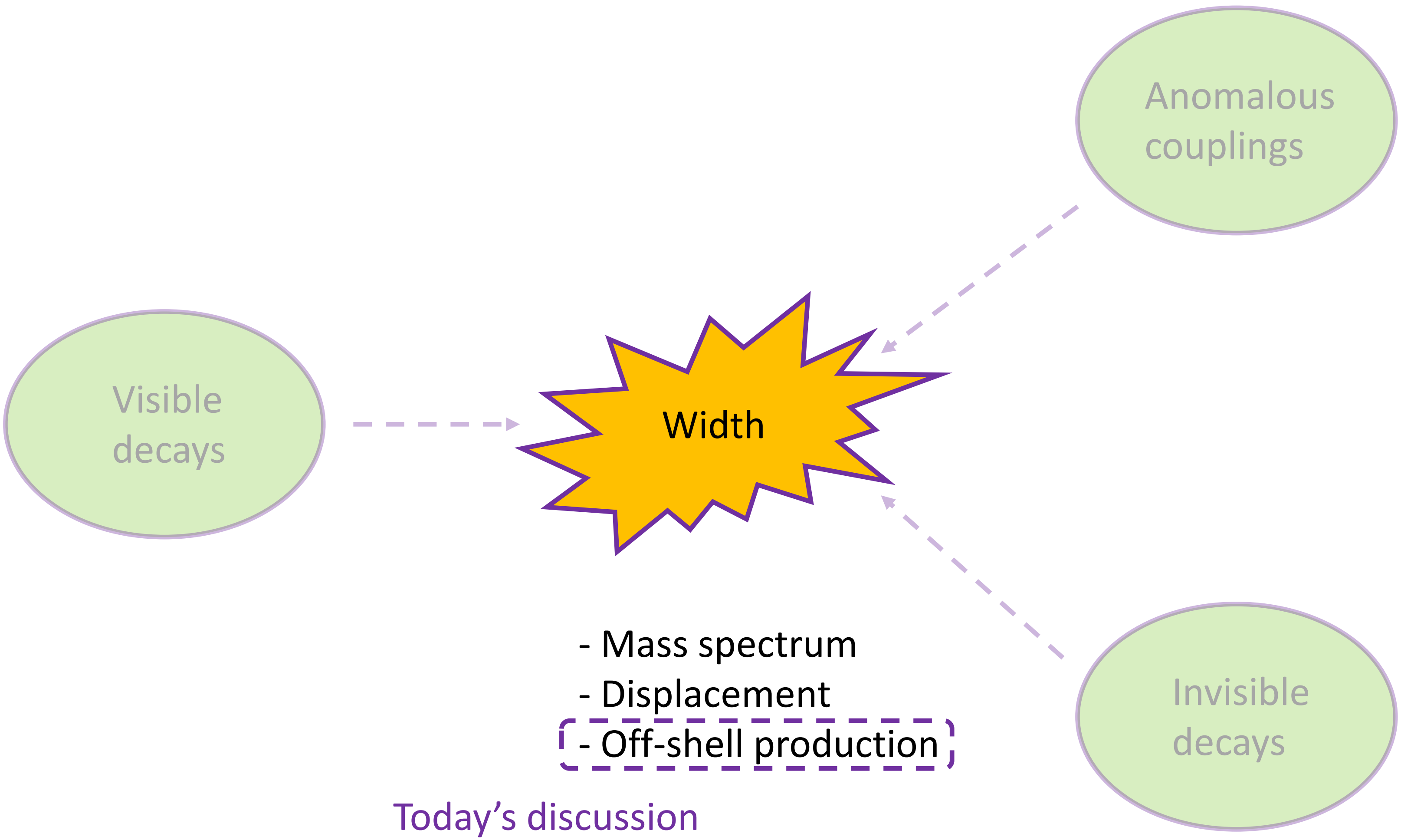

Off-shell Higgs boson production

In $H \rightarrow VV$ ($V = Z, W$), $m_V < m_H < 2m_V$:
→ Either H is on-shell and one V is off-shell, or H is off-shell and both Vs are on-shell

→ Both Vs going on-shell allows ~10% of events in the SM to produce an off-shell Higgs boson [1].

Possible to measure two off-shell production mechanisms:
- $\mu_F^{\text{off-shell}}$ (gg)
- $\mu_V^{\text{off-shell}}$ (EW: VBF, VH)
- Can also measure an overall $\mu^{\text{off-shell}}$

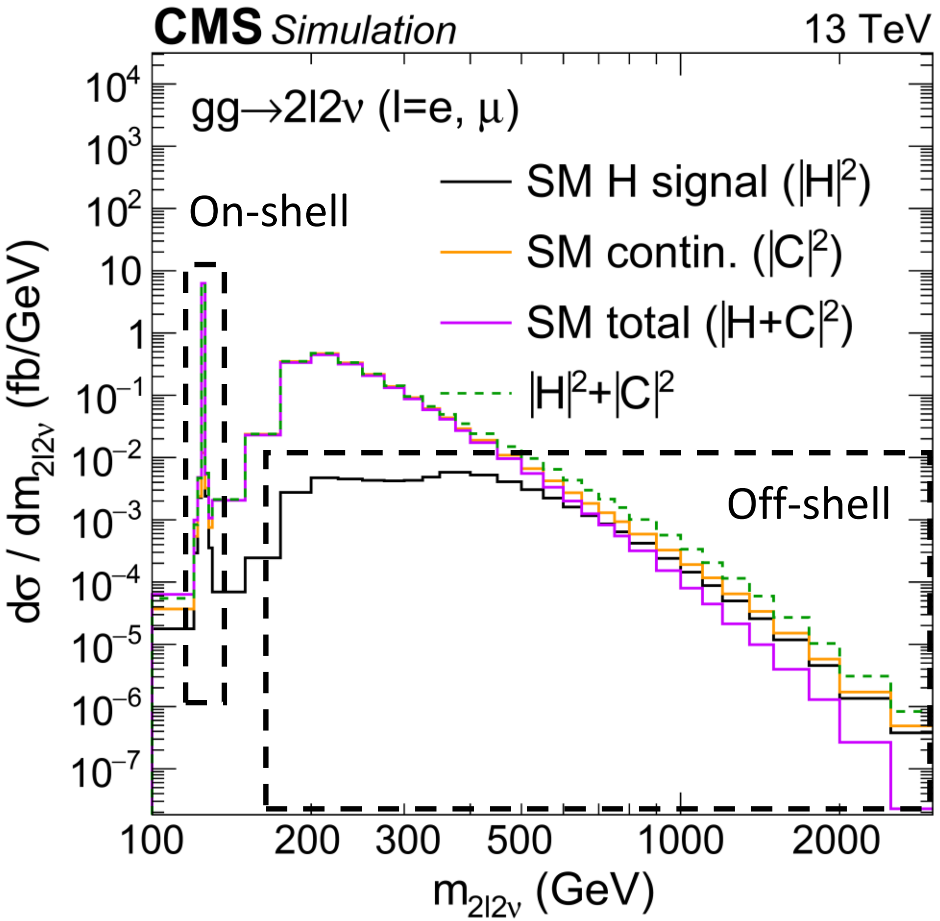

[1] Kauer, N. and Passarino, G.; JHEP 08 116 (2012) (arxiv:1206.4803)

Off-shell Higgs boson production

In $H \rightarrow VV$ $(V = Z, W)$, $m_V < m_H < 2m_V$:
→ Either H is on-shell and one V is off-shell, or H is off-shell and both Vs are on-shell

→ Both Vs going on-shell allows $\sim 10\%$ of events in the SM to produce an off-shell Higgs boson [1].

Possible to measure two off-shell production mechanisms:
- $\mu_F^{\text{off-shell}}$ (gg)
- $\mu_V^{\text{off-shell}}$ (EW: VBF, VH)
- Can also measure an overall $\mu^{\text{off-shell}}$

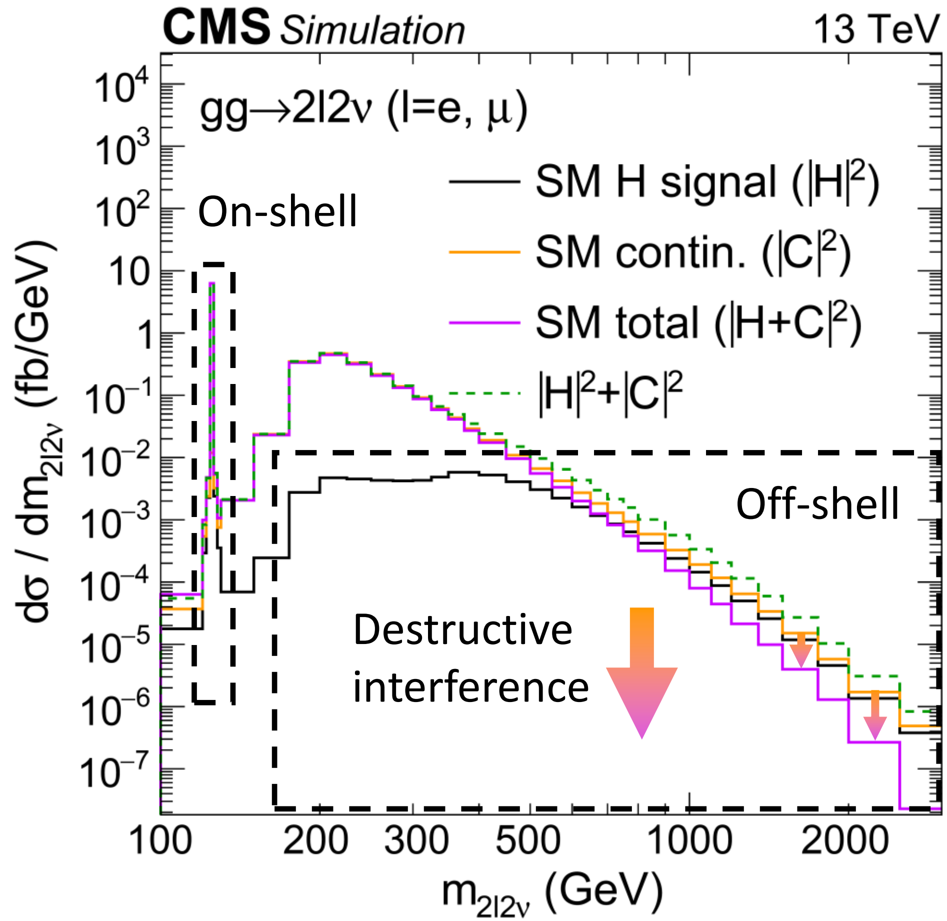

Higgs-mediated diagrams interfere destructively with continuum VV production:
→ Large in magnitude
→ ~Twice the size of the Higgs signal
→ Necessary in the SM to ensure unitarity

[1] Kauer, N. and Passarino, G.; JHEP 08 116 (2012) (arxiv:1206.4803)

Diagrams of off-shell Higgs production

$gg \to H \to ZZ$:

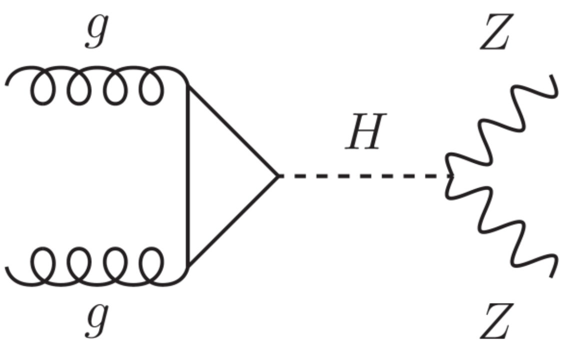

VBF (s-channel):

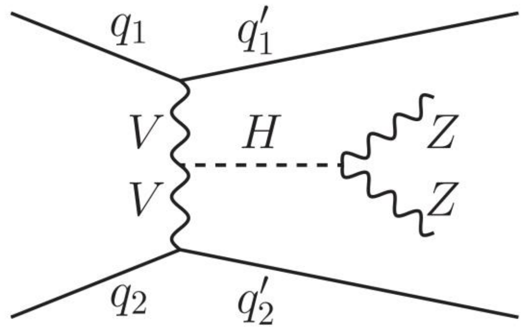

VBF (t-channel):

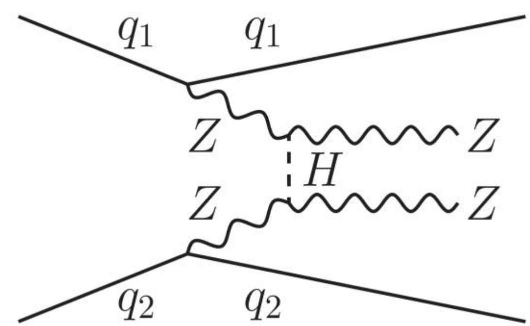

$gg \to H$ production dominant at lower masses in the off-shell region

ZH (s-, t-, u-channels):

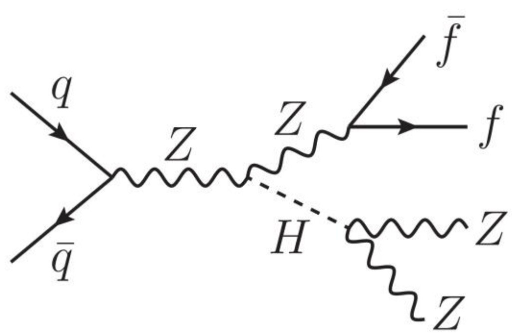

WH:

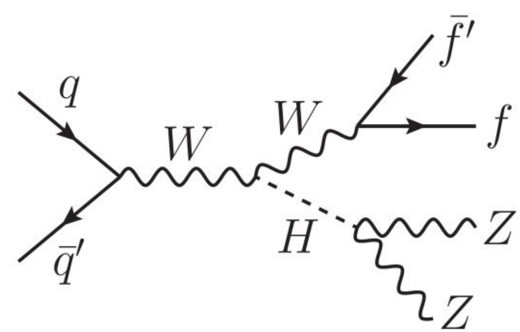

EW production more dominant at higher masses in the off-shell region (mostly VBF in the SM)

Off-shell method for the width

Combine with on-shell signal strength measurement to extract Γ_H [1]:

$$\sigma = \int \frac{g_{prod}^2 g_{dec}^2}{(m^2 - m_\mathrm{H}^2)^2 + m_\mathrm{H}^2 \Gamma_\mathrm{H}^2} \ldots dm^2$$

On-shell

$$\sigma \propto \frac{g_{prod}^2 g_{dec}^2}{\Gamma_\mathrm{H}} \propto \mu_{prod}$$

Measure on-shell signal strength
from final states ZZ or WW

[1] Caola F. and Melnikov, K. PRD 88 054024 (2013)
(arxiv:1307.4935)

Off-shell method for the width

Combine with on-shell signal strength measurement to extract Γ_{H} [1]:

$$\sigma = \int \frac{g_{prod}^2 g_{dec}^2}{(m^2 - m_{\mathrm{H}}^2)^2 + m_{\mathrm{H}}^2 \Gamma_{\mathrm{H}}^2} \ldots dm^2$$

On-shell

$$\sigma \propto \frac{g_{prod}^2 g_{dec}^2}{\Gamma_{\mathrm{H}}} \propto \mu_{prod}$$

Off-shell

$$\sigma \sim \int \frac{g_{prod}^2 g_{dec}^2}{(m^2 - m_{\mathrm{H}}^2)^2} \ldots dm^2 \propto \mu_{prod}^{\mathrm{off-shell}}$$

Measure on-shell signal strength
from final states ZZ or WW

[1] Caola F. and Melnikov, K. PRD 88 054024 (2013) (arxiv:1307.4935)

Off-shell method for the width

Combine with on-shell signal strength measurement to extract Γ_{H} [1]:

$$\sigma = \int \frac{g_{prod}^2 g_{dec}^2}{(m^2 - m_{\mathrm{H}}^2)^2 + m_{\mathrm{H}}^2 \Gamma_{\mathrm{H}}^2} \ldots dm^2$$

On-shell

Off-shell

$$\sigma \propto \frac{g_{prod}^2 g_{dec}^2}{\Gamma_{\mathrm{H}}} \propto \mu_{prod}$$

$$\sigma \sim \int \frac{g_{prod}^2 g_{dec}^2}{(m^2 - m_{\mathrm{H}}^2)^2} \ldots dm^2 \propto \mu_{prod} \cdot \Gamma_{\mathrm{H}}$$

Measure on-shell signal strength from final states ZZ or WW

Ratio of off-shell to on-shell signal strengths for each production mode gives Γ_{H}

[1] Caola F. and Melnikov, K. PRD 88 054024 (2013) (arxiv:1307.4935)

Off-shell & BSM HVV couplings

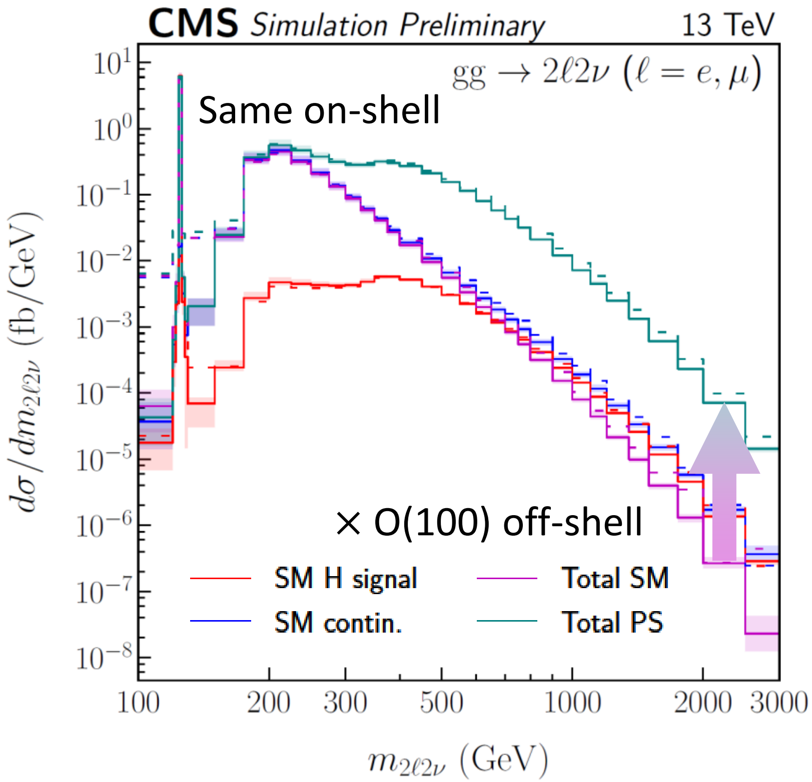

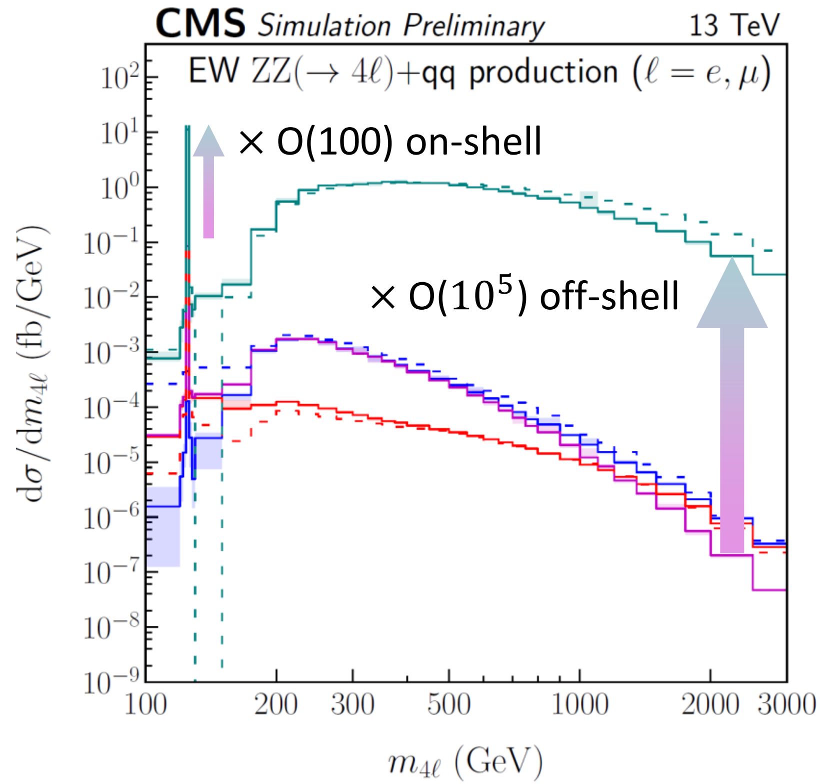

$$A(HVV) \sim \left[\boldsymbol{a_1} - e^{i\phi_{\Lambda 1}} \frac{(q_{V1}^2 + q_{V2}^2)}{\Lambda_1^2} + \cdots \right] m_V^2 \epsilon_{V1}^* \epsilon_{V2}^* + |a_2|\, e^{i\phi_{a2}}\, f_{\mu\nu}^{*(1)} f^{*(2),\mu\nu} + |a_3|\, e^{i\phi_{a3}}\, f_{\mu\nu}^{*(1)} \tilde{f}^{*(2),\mu\nu}$$

HVV amplitude
$\propto \Lambda_1, a_2, a_3$ BSM contributions
+ SM-like a_1 term

Same a_1 (SM) or a_3 (PS) couplings,
different on-shell and off-shell enhancements
in gg and EW production modes

Analysis ingredients

Need high-mass ZZ events that contain off-shell Higgs boson contributions
→ Can be done in both 4ℓ (high-m_{4l}) and $2\ell 2\nu$ (high-m_{T}^{ZZ}) final states
→ $\mathrm{BR}(2\ell 2\nu) \sim 6 \times \mathrm{BR}(4\ell)$
→ 4ℓ cleaner in bkgs. (only irreducible) while $2\ell 2\nu$ also has instrumental components.
→ About equal statistical importance in the results from the two channels

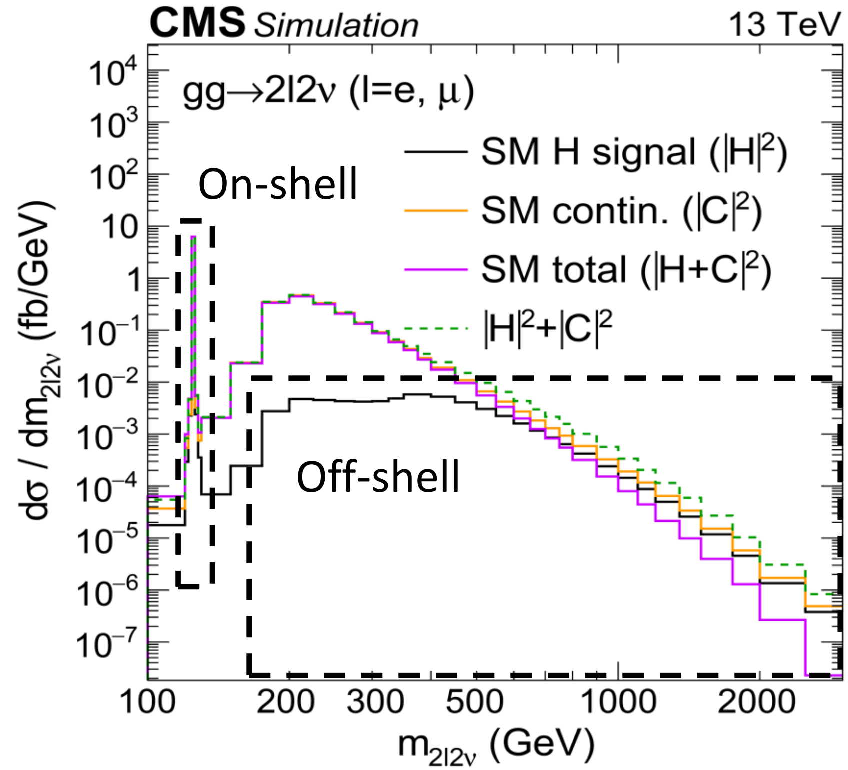

Need on-shell $\mathrm{H}(125)$ events to extract Γ_{H}
→ 4ℓ only (not possible with neutrinos)
→ Little background

Extract physics using a combined fit to 117 multidimensional distributions:
24 distributions in off-shell $2\ell 2\nu$ (2326 events)
→ Analysis also combines 18 distributions from a $WZ \rightarrow 3\ell\nu$ CR (8541 events)
18 distributions in off-shell 4ℓ (1407 events), and 57 distributions in on-shell 4ℓ (621 events)

In off-shell categories, event counts are typically different from the SM by ~10-50% (larger at higher masses) for $\mu^{\mathrm{off-shell}} = 0$ (or ~ 2.5)

Analysis ingredients

Need high-mass ZZ events that contain off-shell Higgs boson contributions
→ Can be done in both 4ℓ (high-m_{4l}) and $2\ell 2\nu$ (high-m_{T}^{ZZ}) final states
→ $\mathrm{BR}(2\ell 2\nu) \sim 6 \times \mathrm{BR}(4\ell)$
→ 4ℓ cleaner in bkgs. (only irreducible) while $2\ell 2\nu$ also has instrumental components.
→ About equal statistical importance in the results from the two channels

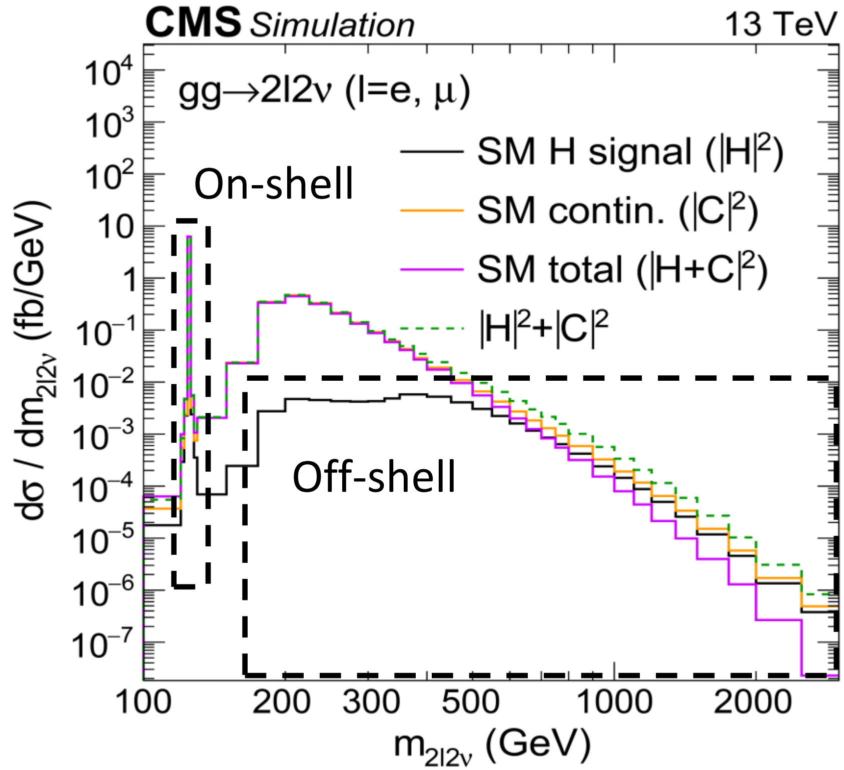

Need on-shell $\mathrm{H}(125)$ events to extract Γ_{H}
→ 4ℓ only (not possible with neutrinos)
→ Little background

Biggest challenge in analysis is to extract off-shell information from the tails:
→ Limited statistics, e.g., in $2\ell 2\nu$ with $N_j \geq 2$, $p_{\mathrm{T}}^{\mathrm{miss}} > 200$ GeV, and $m_{\mathrm{T}}^{ZZ} > 450$ GeV, off-shell $|\mathrm{H}|^2$:H-C interf.:total expected = 10:-17:64 (events)
→ Need precise control over instrumental and irreducible backgrounds
→ Need theory input, e.g. for NLO EW corrections in $q\bar{q} \to ZZ, WZ$, for increased precision

CMS Detector

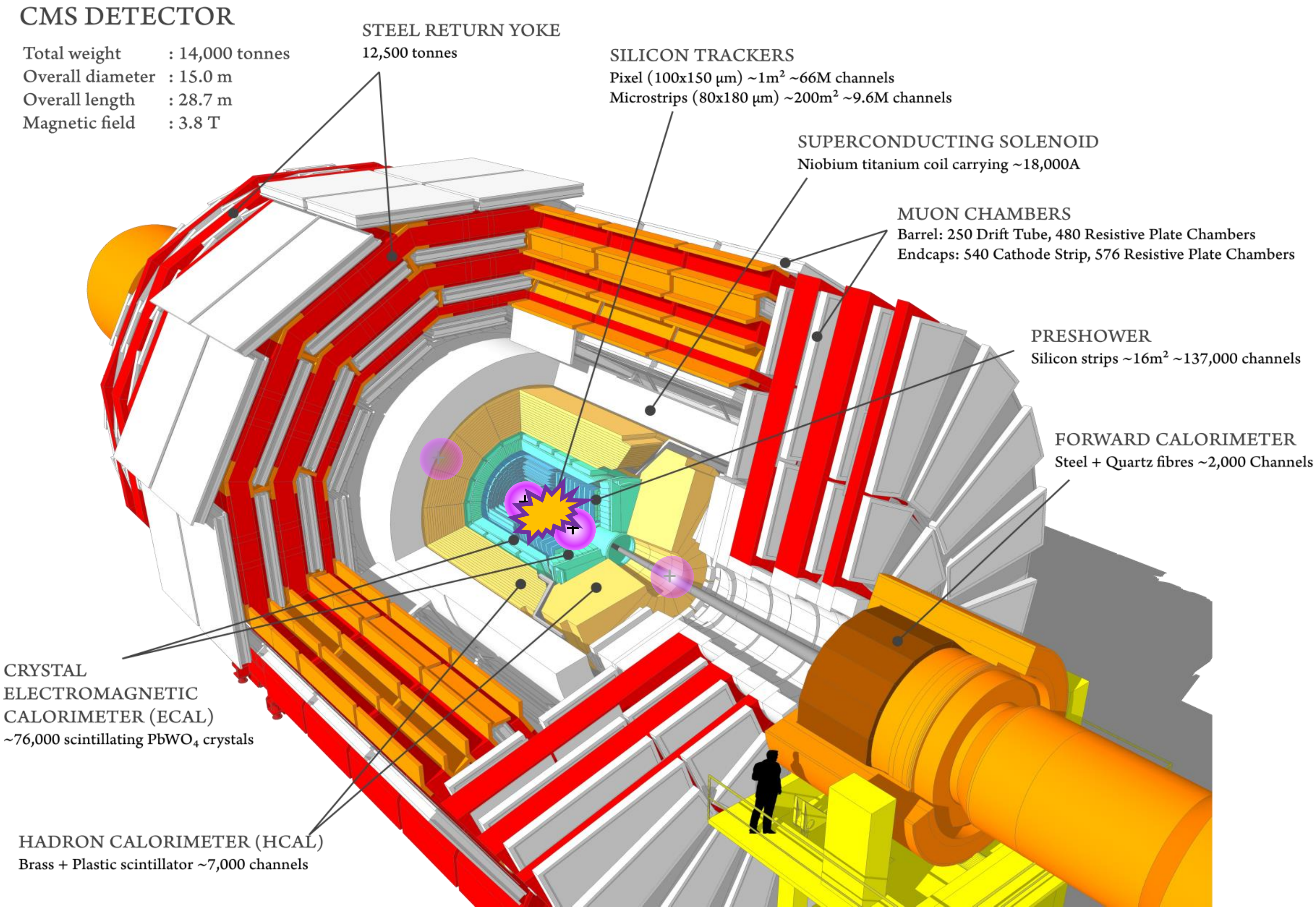

Particle reconstruction in a nutshell

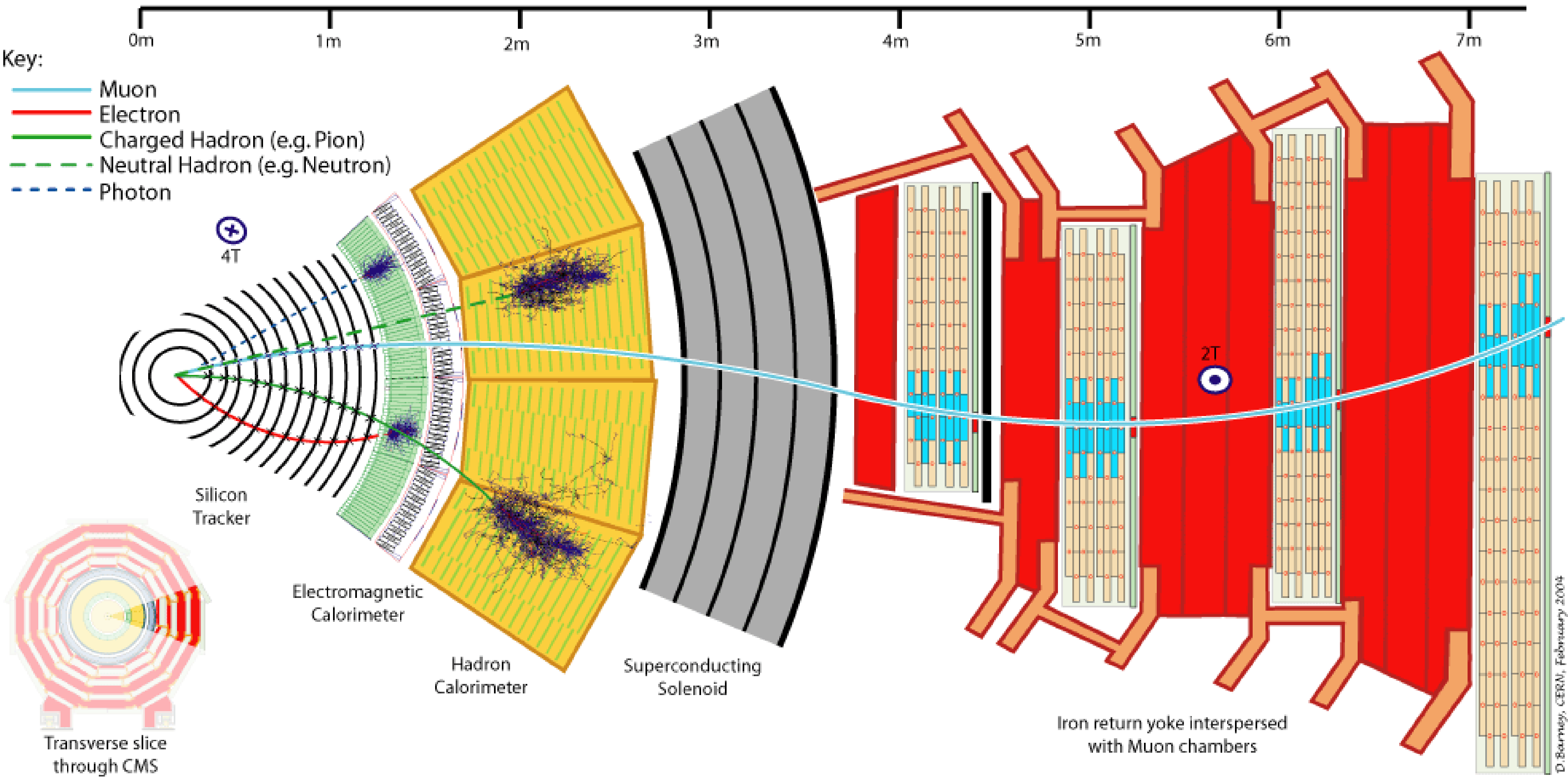

Use particle-flow algorithm [1]:

- Correlate basic detector info. from different layers to identify muons, electrons, photons, and charged and neutral hadrons

PF ID is the basis for particle identification before additional clustering or selection reqs.

[1] CMS Collaboration; JINST 12 P10003 (2017) (arxiv:1706.04965)

Typical lepton efficiencies

Detector is very efficient in reconstructing leptons.
→ Here are exemplary lepton selection efficiencies.

Muons: ~85% – 98%

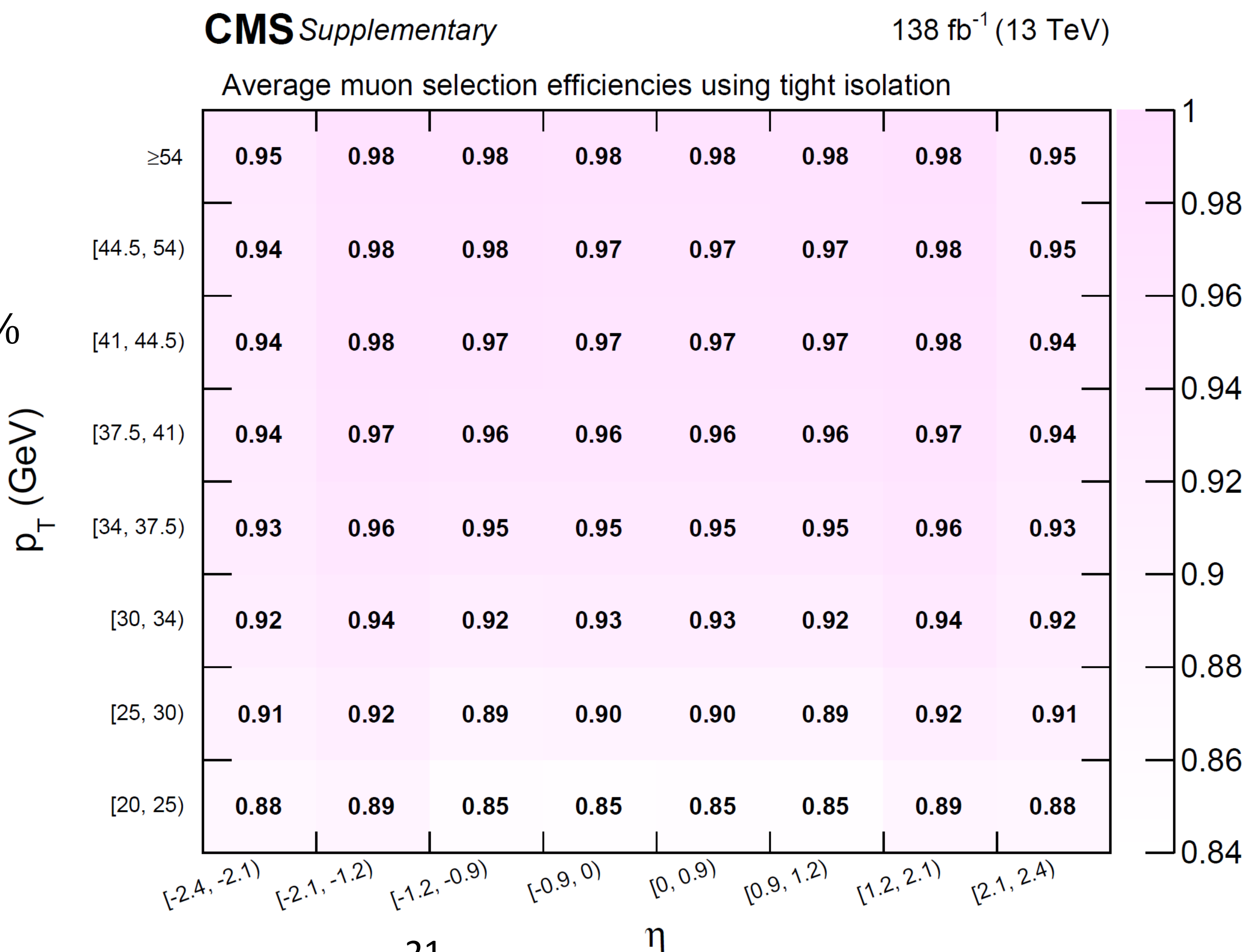

Typical lepton efficiencies

Detector is very efficient in reconstructing leptons.
→ Here are exemplary lepton selection efficiencies.

Electrons: ~48% − 88%

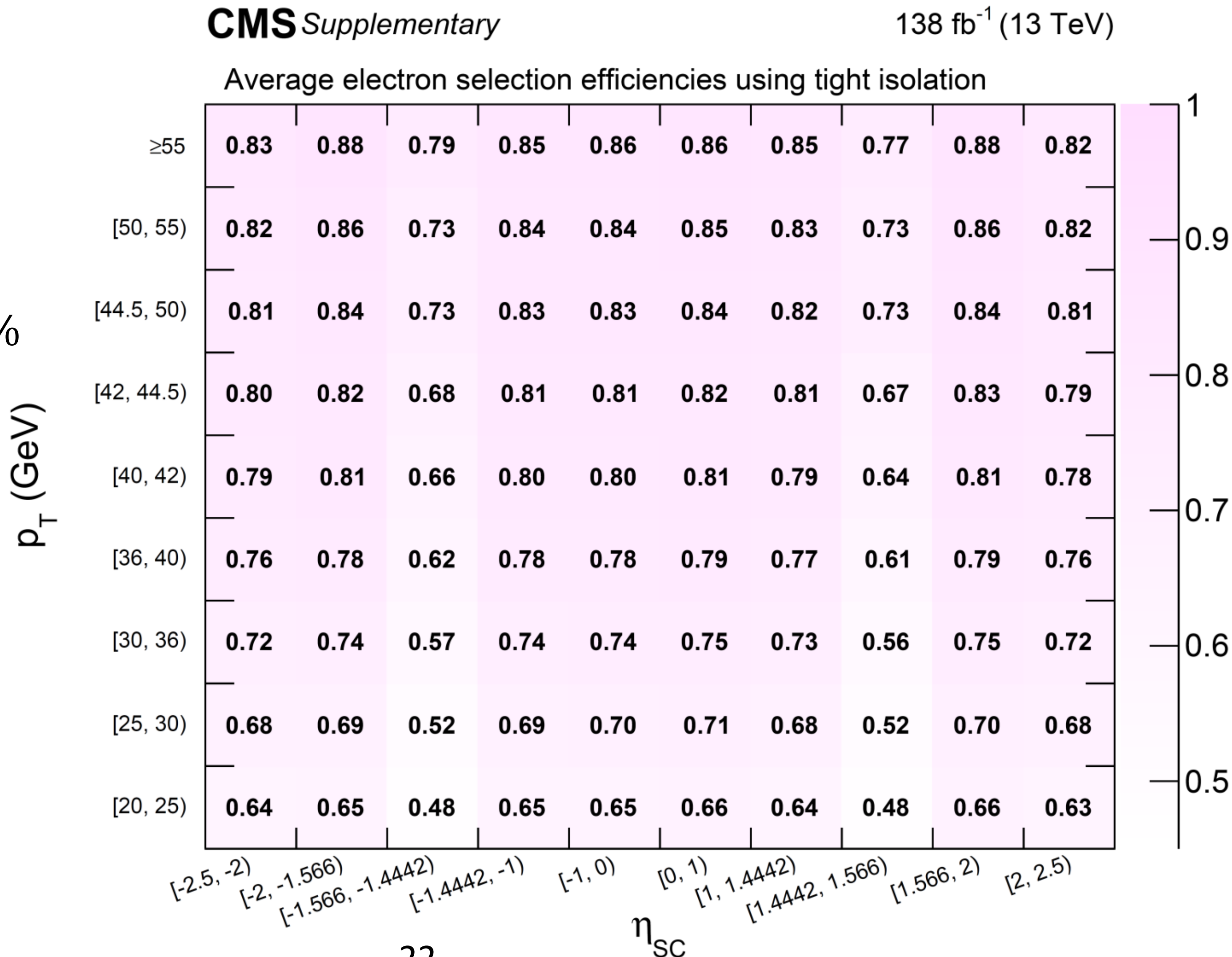

Transverse momentum of neutrinos

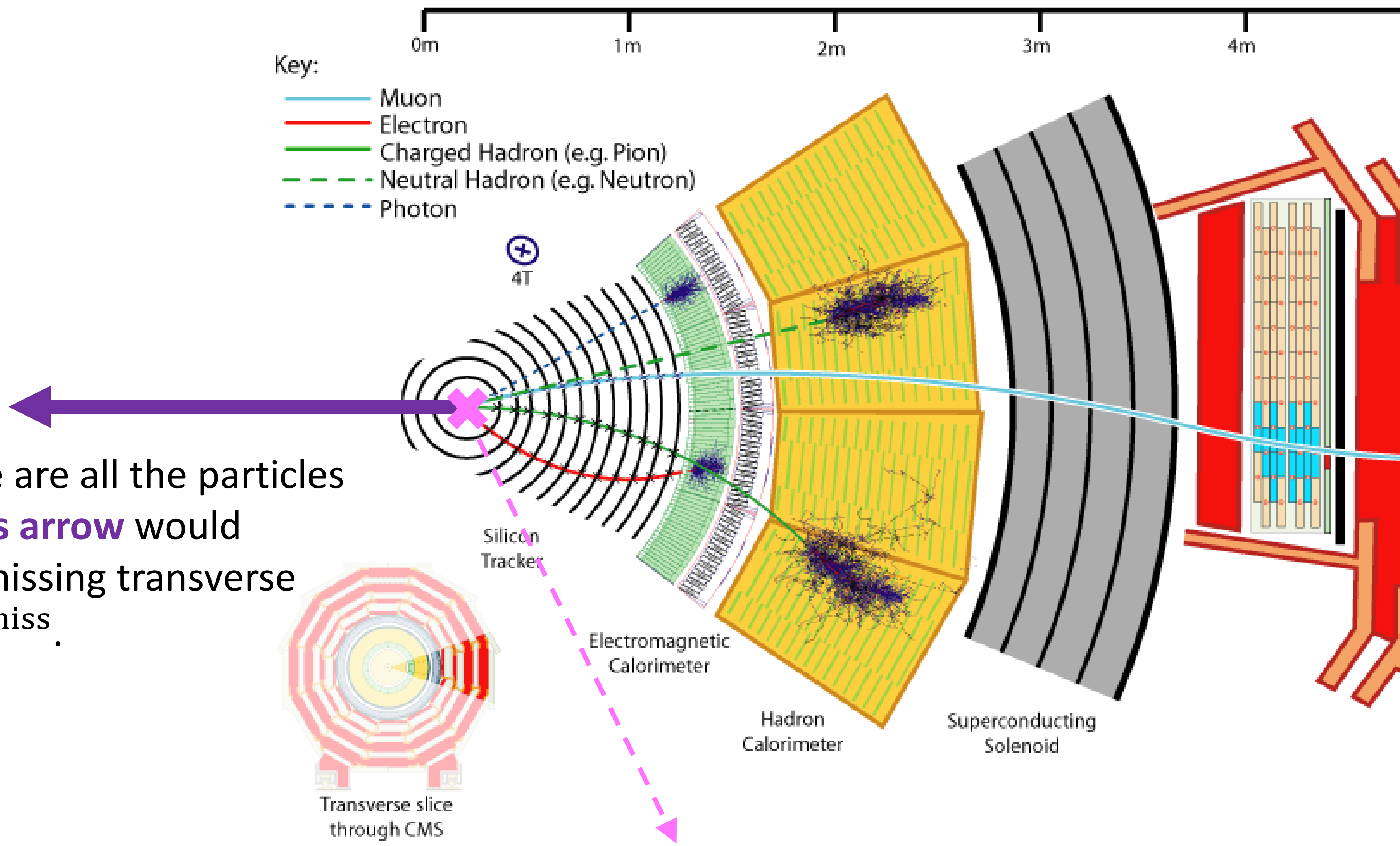

Assuming these are all the particles in an event, **this arrow** would represent the missing transverse momentum, $p_{\mathrm{T}}^{\mathrm{miss}}$.

Total transverse momentum from the collision should be 0.

Off-shell 4ℓ: Analysis strategy

CMS-HIG-18-002: Analysis of off-shell ($m_{4l} > 220$ GeV) 2016+2017 data [1]
→ All momenta are known in 4ℓ ⇒ Use MELA matrix element discriminants
→ Can compute for Higgs production, decay, or both; or backgrounds

$$\mathcal{D}_{\rm alt}\left(\mathbf{\Omega}\right) = \frac{\mathcal{P}_{\rm sig}\left(\mathbf{\Omega}\right)}{\mathcal{P}_{\rm sig}\left(\mathbf{\Omega}\right) + \mathcal{P}_{\rm alt}\left(\mathbf{\Omega}\right)}$$

sig. vs alt.

$$\mathcal{D}_{\rm int}\left(\mathbf{\Omega}\right) = \frac{\mathcal{P}_{\rm int}\left(\mathbf{\Omega}\right)}{2\sqrt{\mathcal{P}_{\rm sig}\left(\mathbf{\Omega}\right)\ \mathcal{P}_{\rm alt}\left(\mathbf{\Omega}\right)}}$$

sig.-alt. interference

[1] CMS Collaboration; PRD 99 112003 (2019) (arxiv:1901.00174)

Off-shell 4ℓ: Analysis strategy

CMS-HIG-18-002: Analysis of off-shell ($m_{4l} > 220$ GeV) 2016+2017 data [1]
→ All momenta are known in 4ℓ ⇒ Use MELA matrix element discriminants
→ Can compute for Higgs production, decay, or both; or backgrounds

$$\mathcal{D}_{\text{alt}}(\boldsymbol{\Omega}) = \frac{\mathcal{P}_{\text{sig}}(\boldsymbol{\Omega})}{\mathcal{P}_{\text{sig}}(\boldsymbol{\Omega}) + \mathcal{P}_{\text{alt}}(\boldsymbol{\Omega})}$$

sig. vs alt.

$$\mathcal{D}_{\text{int}}(\boldsymbol{\Omega}) = \frac{\mathcal{P}_{\text{int}}(\boldsymbol{\Omega})}{2\sqrt{\mathcal{P}_{\text{sig}}(\boldsymbol{\Omega})\ \mathcal{P}_{\text{alt}}(\boldsymbol{\Omega})}}$$

sig.-alt. interference

Category	VBF-tagged	VH-tagged	Untagged
Selection	$\mathcal{D}_{\text{2jet}}^{\text{VBF}}$ or $\mathcal{D}_{\text{2jet}}^{\text{VBF,BSM}} > 0.5$	$\mathcal{D}_{\text{2jet}}^{\text{WH}}$ or $\mathcal{D}_{\text{2jet}}^{\text{WH,BSM}}$, or $\mathcal{D}_{\text{2jet}}^{\text{ZH}}$ or $\mathcal{D}_{\text{2jet}}^{\text{ZH,BSM}} > 0.5$	Rest of events
SM obs.	$m_{4\ell}$, $\mathcal{D}_{\text{bkg}}^{\text{VBF+dec}}$, $\mathcal{D}_{\text{bsi}}^{\text{VBF+dec}}$	$m_{4\ell}$, $\mathcal{D}_{\text{bkg}}^{\text{VH+dec}}$, $\mathcal{D}_{\text{bsi}}^{\text{VH+dec}}$	$m_{4\ell}$, $\mathcal{D}_{\text{bkg}}^{\text{kin}}$, $\mathcal{D}_{\text{bsi}}^{\text{gg,dec}}$

Mass shape is the most sensitive to off-shell production
→ Any off-shell analysis uses a mass-sensitive observable

[1] CMS Collaboration; PRD 99 112003 (2019) (arxiv:1901.00174)

Off-shell 4ℓ: Analysis strategy

CMS-HIG-18-002: Analysis of off-shell ($m_{4l} > 220$ GeV) 2016+2017 data [1]
→ All momenta are known in 4ℓ ⇒ Use MELA matrix element discriminants
→ Can compute for Higgs production, decay, or both; or backgrounds

$$\mathcal{D}_{\mathrm{alt}}(\mathbf{\Omega}) = \frac{\mathcal{P}_{\mathrm{sig}}(\mathbf{\Omega})}{\mathcal{P}_{\mathrm{sig}}(\mathbf{\Omega}) + \mathcal{P}_{\mathrm{alt}}(\mathbf{\Omega})}$$

sig. vs alt.

$$\mathcal{D}_{\mathrm{int}}(\mathbf{\Omega}) = \frac{\mathcal{P}_{\mathrm{int}}(\mathbf{\Omega})}{2\sqrt{\mathcal{P}_{\mathrm{sig}}(\mathbf{\Omega})\ \mathcal{P}_{\mathrm{alt}}(\mathbf{\Omega})}}$$

sig.-alt. interference

Category	VBF-tagged	VH-tagged	Untagged
Selection	$\mathcal{D}_{\mathrm{2jet}}^{\mathrm{VBF}}$ or $\mathcal{D}_{\mathrm{2jet}}^{\mathrm{VBF,BSM}} > 0.5$	$\mathcal{D}_{\mathrm{2jet}}^{\mathrm{WH}}$ or $\mathcal{D}_{\mathrm{2jet}}^{\mathrm{WH,BSM}}$, or $\mathcal{D}_{\mathrm{2jet}}^{\mathrm{ZH}}$ or $\mathcal{D}_{\mathrm{2jet}}^{\mathrm{ZH,BSM}} > 0.5$	Rest of events
SM obs.	$m_{4\ell}$, $\mathcal{D}_{\mathrm{bkg}}^{\mathrm{VBF+dec}}$, $\mathcal{D}_{\mathrm{bsi}}^{\mathrm{VBF+dec}}$	$m_{4\ell}$, $\mathcal{D}_{\mathrm{bkg}}^{\mathrm{VH+dec}}$, $\mathcal{D}_{\mathrm{bsi}}^{\mathrm{VH+dec}}$	$m_{4\ell}$, $\mathcal{D}_{\mathrm{bkg}}^{\mathrm{kin}}$, $\mathcal{D}_{\mathrm{bsi}}^{\mathrm{gg,dec}}$

Mass shape is the most sensitive to off-shell production
→ Any off-shell analysis uses a mass-sensitive observable

+ Discriminant for signal vs bkg
+ Discriminant for Higgs-continuum ZZ interference
  (or SM vs BSM if constraining anomalous couplings)

[1] CMS Collaboration; PRD 99 112003 (2019) (arxiv:1901.00174)

Off-shell 4ℓ: Event distributions

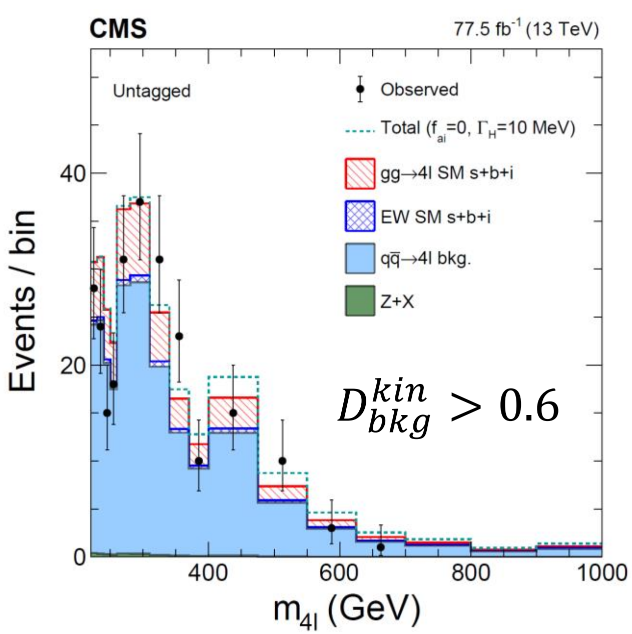

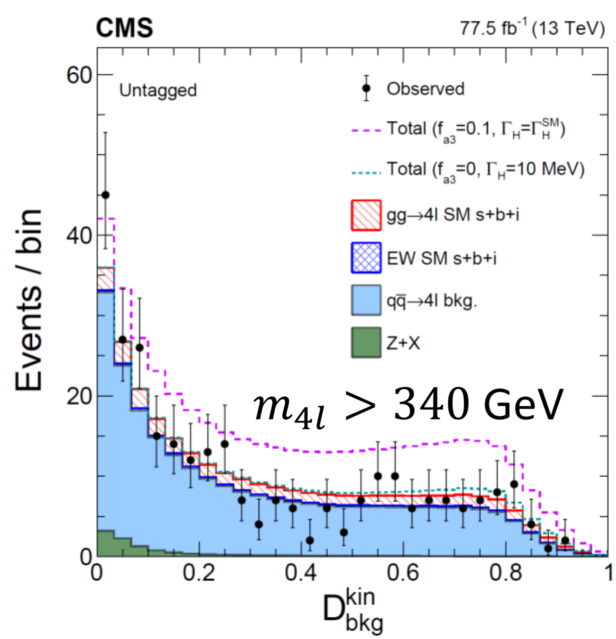

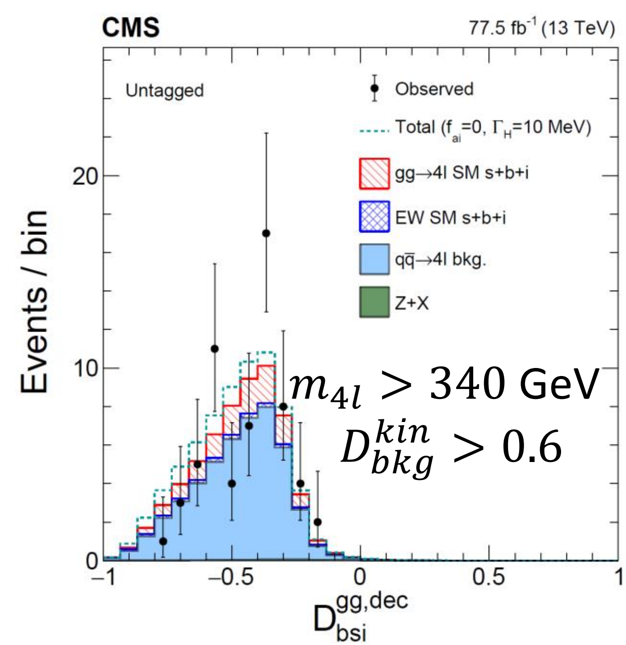

Example distributions from the untagged category

Selection requirements are applied on the plots
to enhance Higgs contributions

Stacked histograms for prefit SM distributions ($\Gamma_{\rm H} = 4.1$ MeV),
cyan for $\Gamma_{\rm H} = 10$ MeV, magenta for an on-shell 10% PS (a_3) mixture

On-shell 4ℓ: Analysis strategy

CMS-HIG-19-009: Analysis of on-shell 4ℓ 2016-2018 data [1]

→ Utilizes a finer categorization and more discriminants as observables

→ Same categorization and observables for all couplings

→ Example from untagged category:

$$\mathcal{D}_{\rm bkg}, \mathcal{D}_{0h+}^{\rm dec}, \mathcal{D}_{0-}^{\rm dec}, \mathcal{D}_{\Lambda1}^{\rm dec}, \mathcal{D}_{\Lambda1}^{Z\gamma,\rm dec}, \mathcal{D}_{\rm int}^{\rm dec}, \mathcal{D}_{CP}^{\rm dec}$$

SM vs BSM — SM-BSM interf.

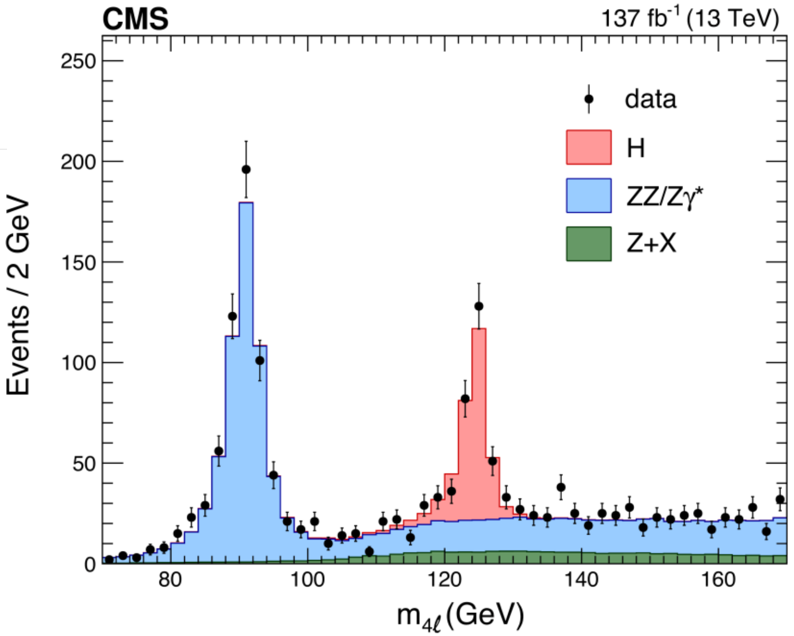

Provides extensive set of results

→ Provides the following input to off-shell analysis:

on-shell μ_F and μ_V

on-shell BSM HVV contribution fractions f_{ai}

[1] CMS Collaboration; PRD 104 052004 (2021) (arxiv:2104.12152)

On-shell 4ℓ: Analysis strategy

CMS-HIG-19-009: Analysis of on-shell 4ℓ 2016-2018 data [1]

→ Utilizes a finer categorization and more discriminants as observables

→ Same categorization and observables for all couplings

→ Example from untagged category:

$$\mathcal{D}_{\rm bkg}, \mathcal{D}_{0h+}^{\rm dec}, \mathcal{D}_{0-}^{\rm dec}, \mathcal{D}_{\Lambda1}^{\rm dec}, \mathcal{D}_{\Lambda1}^{Z\gamma,\rm dec}, \mathcal{D}_{\rm int}^{\rm dec}, \mathcal{D}_{CP}^{\rm dec}$$

SM vs BSM   SM-BSM interf.

Provides extensive set of results

→ Provides the following input to off-shell analysis:

on-shell μ_F and μ_V

on-shell BSM HVV contribution fractions f_{ai}

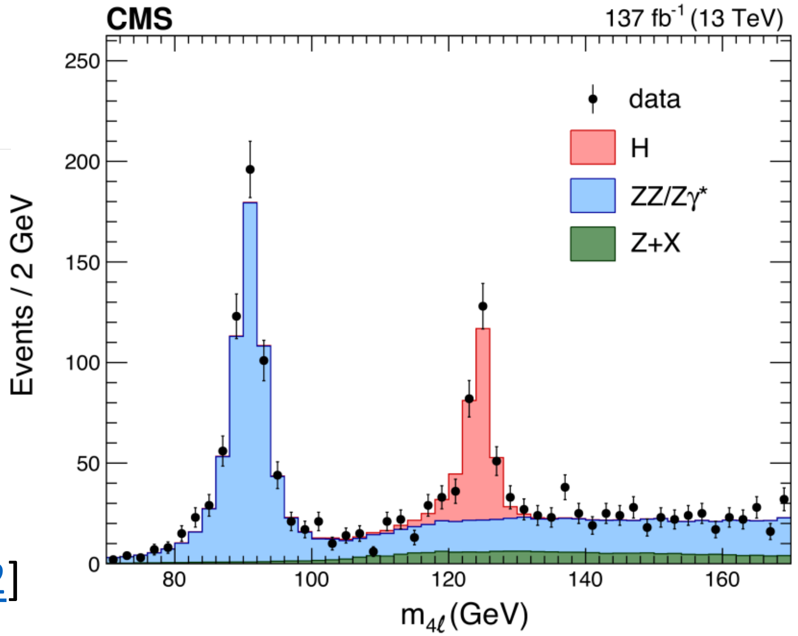

CMS-HIG-17-011: Analysis of on-shell 4ℓ 2015 data [2]

→ Inclusive in categorization

→ Observables: $D_{bkg}, D_{BSM}^{dec}, D_{int}^{dec}$ as in the untagged category above.

→ The BSM discriminant depends on the analyzed coupling.

[1] PRD 104 052004 (2021) (arxiv:2104.12152)

[2] PLB 775 1 (2017) (arxiv:1707.00541)

Off-shell $2\ell 2\nu$: Analysis strategy

CMS-HIG-21-013: Analysis of off-shell $\mathrm{ZZ} \to 2\ell 2\nu$ 2016-2018 data [1]

→ Main observable: Transverse ZZ mass defined through

$$m_{\mathrm{T}}^{\mathrm{ZZ}\,2} = \left[\sqrt{p_{\mathrm{T}}^{\ell\ell\,2} + m_{\ell\ell}{}^{2}} + \sqrt{p_{\mathrm{T}}^{\mathrm{miss}\,2} + m_{\mathrm{Z}}{}^{2}} \right]^{2} - \left| \vec{p}_{\mathrm{T}}^{\,\ell\ell} + \vec{p}_{\mathrm{T}}^{\,\mathrm{miss}} \right|^{2}$$

→ $p_{\mathrm{T}}^{\mathrm{miss}}$ also used as an observable since it is sensitive to backgrounds

[1] CMS Collaboration; Nature Phys. 18 11 (2022) (arxiv:2202.06923)

Off-shell $2\ell 2\nu$: Analysis strategy

CMS-HIG-21-013: Analysis of off-shell $\mathrm{ZZ} \to 2\ell 2\nu$ 2016-2018 data [1]

→ Main observable: Transverse ZZ mass defined through

$$m_{\mathrm{T}}^{\mathrm{ZZ}^2} = \left[\sqrt{p_{\mathrm{T}}^{\ell\ell^2} + m_{\ell\ell}{}^2} + \sqrt{p_{\mathrm{T}}^{\mathrm{miss}^2} + m_{\mathrm{Z}}{}^2} \right]^2 - \left| \vec{p}_{\mathrm{T}}^{\,\ell\ell} + \vec{p}_{\mathrm{T}}^{\,\mathrm{miss}} \right|^2$$

→ $p_{\mathrm{T}}^{\mathrm{miss}}$ also used as an observable since it is sensitive to backgrounds

→ Categorization in bins of the number of jets: $N_j = 0, 1, \geq 2$

→ Also uses the MELA discriminants $D_{2jet}^{VBF(,BSM)}$ when $N_j \geq 2$ by assuming $\eta_{\nu\nu} = \eta_{\ell\ell}$

[1] CMS Collaboration; Nature Phys. 18 11 (2022) (arxiv:2202.06923)

Off-shell $2\ell 2\nu$: Analysis strategy

CMS-HIG-21-013: Analysis of off-shell $ZZ \to 2\ell 2\nu$ 2016-2018 data [1]

→ Main observable: Transverse ZZ mass defined through

$$m_{\mathrm{T}}^{ZZ^2} = \left[\sqrt{p_{\mathrm{T}}^{\ell\ell^2} + m_{\ell\ell}^2} + \sqrt{p_{\mathrm{T}}^{\mathrm{miss}^2} + m_{Z}^2}\right]^2 - \left|\vec{p}_{\mathrm{T}}^{\,\ell\ell} + \vec{p}_{\mathrm{T}}^{\,\mathrm{miss}}\right|^2$$

→ $p_{\mathrm{T}}^{\mathrm{miss}}$ also used as an observable since it is sensitive to backgrounds

→ Categorization in bins of the number of jets: $N_j = 0, 1, \geq 2$

→ Also uses the MELA discriminants $D_{2jet}^{VBF(,BSM)}$ when $N_j \geq 2$ by assuming $\eta_{\nu\nu} = \eta_{\ell\ell}$

Interpretation parameters	$N_j < 2$	$N_j \geq 2$
$\mu_F^{\mathrm{off-shell}}, \mu_V^{\mathrm{off-shell}}, \mu^{\mathrm{off-shell}}$	$m_{\mathrm{T}}^{ZZ}, p_{\mathrm{T}}^{\mathrm{miss}}$	$m_{\mathrm{T}}^{ZZ}, p_{\mathrm{T}}^{\mathrm{miss}}, D_{2jet}^{VBF}, D_{2jet}^{VBF,a2}$
Γ_{H} ($f_{ai} = 0$)	$m_{\mathrm{T}}^{ZZ}, p_{\mathrm{T}}^{\mathrm{miss}}$	$m_{\mathrm{T}}^{ZZ}, p_{\mathrm{T}}^{\mathrm{miss}}, D_{2jet}^{VBF}, D_{2jet}^{VBF,a2}$
$\Gamma_{\mathrm{H}}, f_{a2}$	$m_{\mathrm{T}}^{ZZ}, p_{\mathrm{T}}^{\mathrm{miss}}$	$m_{\mathrm{T}}^{ZZ}, p_{\mathrm{T}}^{\mathrm{miss}}, D_{2jet}^{VBF}, D_{2jet}^{VBF,a2}$
$\Gamma_{\mathrm{H}}, f_{a3}$	$m_{\mathrm{T}}^{ZZ}, p_{\mathrm{T}}^{\mathrm{miss}}$	$m_{\mathrm{T}}^{ZZ}, p_{\mathrm{T}}^{\mathrm{miss}}, D_{2jet}^{VBF}, D_{2jet}^{VBF,a3}$
$\Gamma_{\mathrm{H}}, f_{\Lambda 1}$	$m_{\mathrm{T}}^{ZZ}, p_{\mathrm{T}}^{\mathrm{miss}}$	$m_{\mathrm{T}}^{ZZ}, p_{\mathrm{T}}^{\mathrm{miss}}, D_{2jet}^{VBF}, D_{2jet}^{VBF,\Lambda 1}$

[1] CMS Collaboration; Nature Phys. 18 11 (2022) (arxiv:2202.06923)

Off-shell $2\ell 2\nu$: Noninterfering backgrounds

$q\bar{q} \rightarrow ZZ, WZ$:
→ Dominant backgrounds at high m_{T}^{ZZ}
→ Shapes and normalizations taken from all possible variations of the simulation
→ Final estimate performed with a joint fit to a 3ℓ WZ CR

$q\bar{q} \to ZZ, WZ$ background

$q\bar{q} \to ZZ$ is an irreducible background to $H \to ZZ$
→ $2\ell 2\nu$ also picks up lost-lepton contributions from $q\bar{q}' \to WZ$

Estimation strategy: MC-based with data handle
→ Select a $3\ell + p_{\mathrm{T}}^{\mathrm{miss}}$ sample of WZ prod.
  → Has minimal Higgs contribution
→ Kinematic behavior of ZZ and WZ similar
→ Take shapes and common uncertainties from simulation
→ Calibrate signal region MC shapes using a joint fit with this control sample

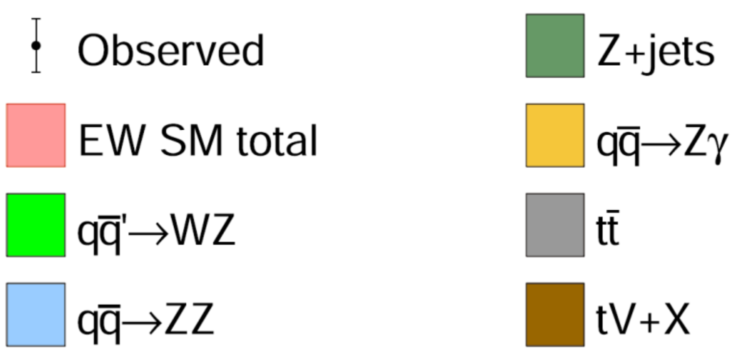

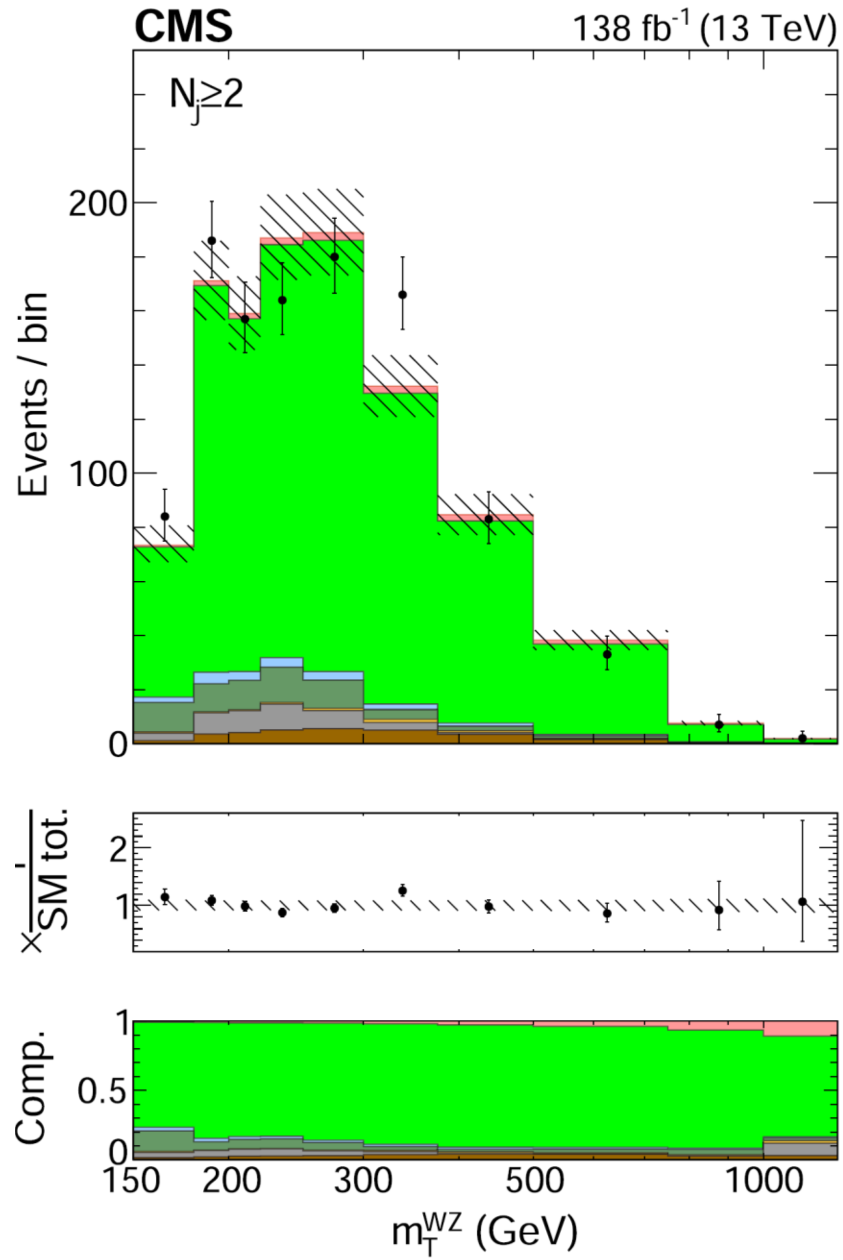

Off-shell $2\ell 2\nu$: Noninterfering backgrounds

$q\bar{q} \to ZZ, WZ$:
→ Dominant backgrounds at high m_{T}^{ZZ}
→ Shapes and normalizations taken from all possible variations of the simulation
→ Final estimate performed with a joint fit to a 3ℓ WZ CR

Instrumental $p_{\mathrm{T}}^{\mathrm{miss}}$:
→ Comes primarily from the $p_{\mathrm{T}}^{\mathrm{miss}}$ tail of Z+jets
→ Estimated from the single-photon CR by reweighting photons to $Z \to \ell\ell$

Instrumental p_T^{miss}

$Z(\rightarrow \ell\ell)$+jets events with large cross section can contaminate the signal region when there are mismeasured jets or large unclustered energy.
→ Small smearing and tight selection, but event rate is high.

Estimation strategy: Data-driven
→ Select γ+jets data to model p_T^{miss} response
→ Calibrate γ kinematics to those for the Z
→ Subtract real-p_T^{miss} processes (histograms up to $Z(\rightarrow \nu\nu)\gamma$)

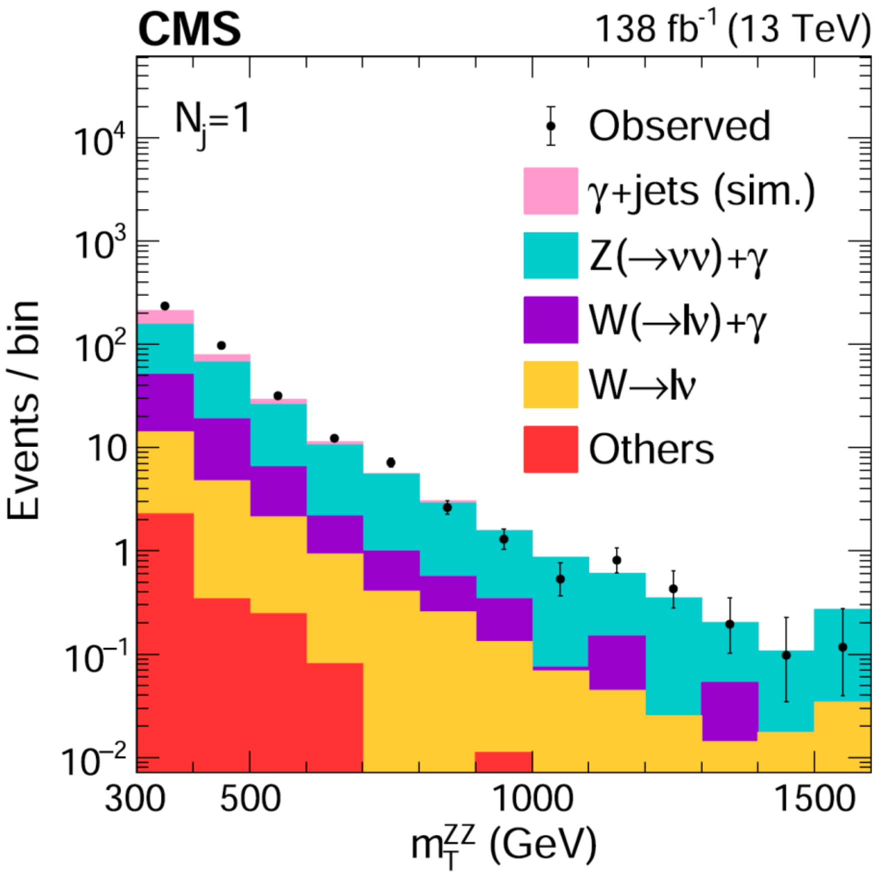

Off-shell $2\ell 2\nu$: Noninterfering backgrounds

$q\bar{q} \to ZZ, WZ$:
→ Dominant backgrounds at high m_{T}^{ZZ}
→ Shapes and normalizations taken from all possible variations of the simulation
→ Final estimate performed with a joint fit to a 3ℓ WZ CR

Instrumental $p_{\mathrm{T}}^{\mathrm{miss}}$:
→ Comes primarily from the $p_{\mathrm{T}}^{\mathrm{miss}}$ tail of Z+jets
→ Estimated from the single-photon CR by reweighting photons to $Z \to \ell\ell$

Nonresonant ($t\bar{t}, WW$):
→ Estimated from reweighting $e\mu$ events for trigger and lepton efficiencies

Nonresonant ($t\bar{t}$, WW) background

SR has non-$Z(\rightarrow \ell\ell)$ contributions with a real $\ell\ell$ pair (fully leptonic $t\bar{t}, WW$ decays).

Estimation strategy: Data-driven

→ Pick $e\mu$ events with otherwise identical reqs.

→ Rate of $e\mu$ = 2 × rate of ee or $\mu\mu$

→ Reweight for lepton and trigger efficiencies to reproduce ee and $\mu\mu$ behavior

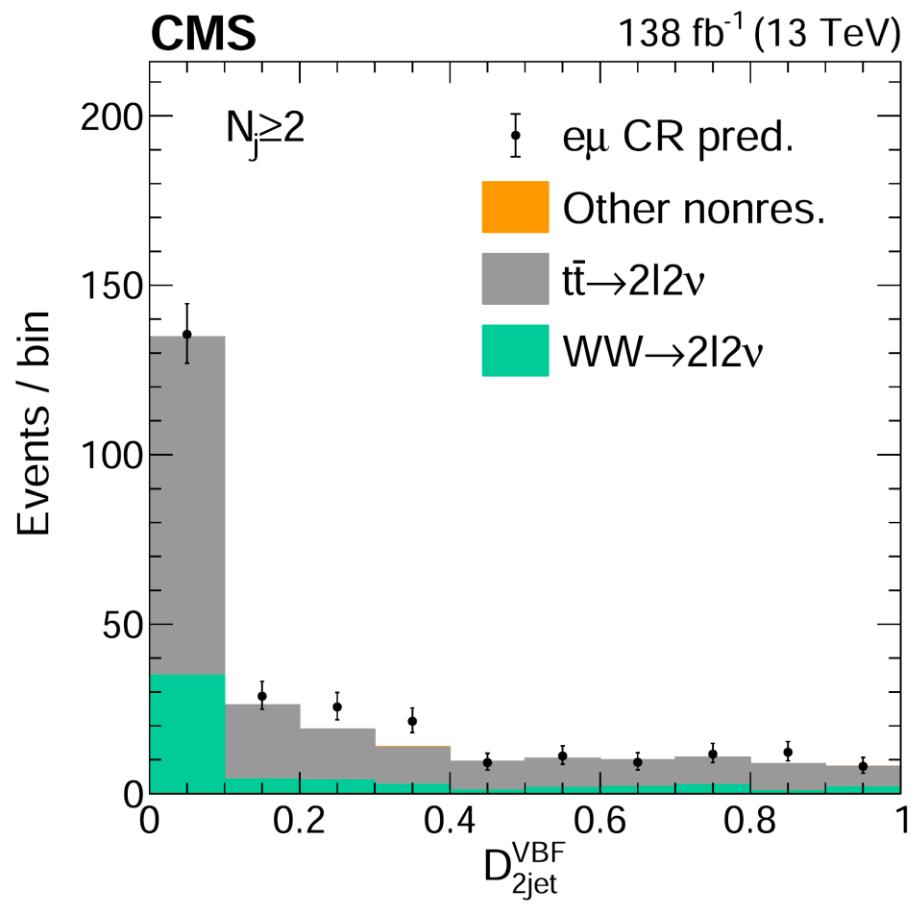

Off-shell $2\ell 2\nu$: Noninterfering backgrounds

$q\bar{q} \to ZZ, WZ$:
→ Dominant backgrounds at high m_{T}^{ZZ}
→ Shapes and normalizations taken from all possible variations of the simulation
→ Final estimate performed with a joint fit to a 3ℓ WZ CR

Instrumental $p_{\mathrm{T}}^{\mathrm{miss}}$:
→ Comes primarily from the $p_{\mathrm{T}}^{\mathrm{miss}}$ tail of Z+jets
→ Estimated from the single-photon CR by reweighting photons to $Z \to \ell\ell$

Nonresonant ($t\bar{t}, WW$):
→ Estimated from reweighting $e\mu$ events for trigger and lepton efficiencies

$tZ + X$:
→ Minor contribution
→ Estimated fully from simulation

Off-shell $2\ell2\nu$: Event distributions

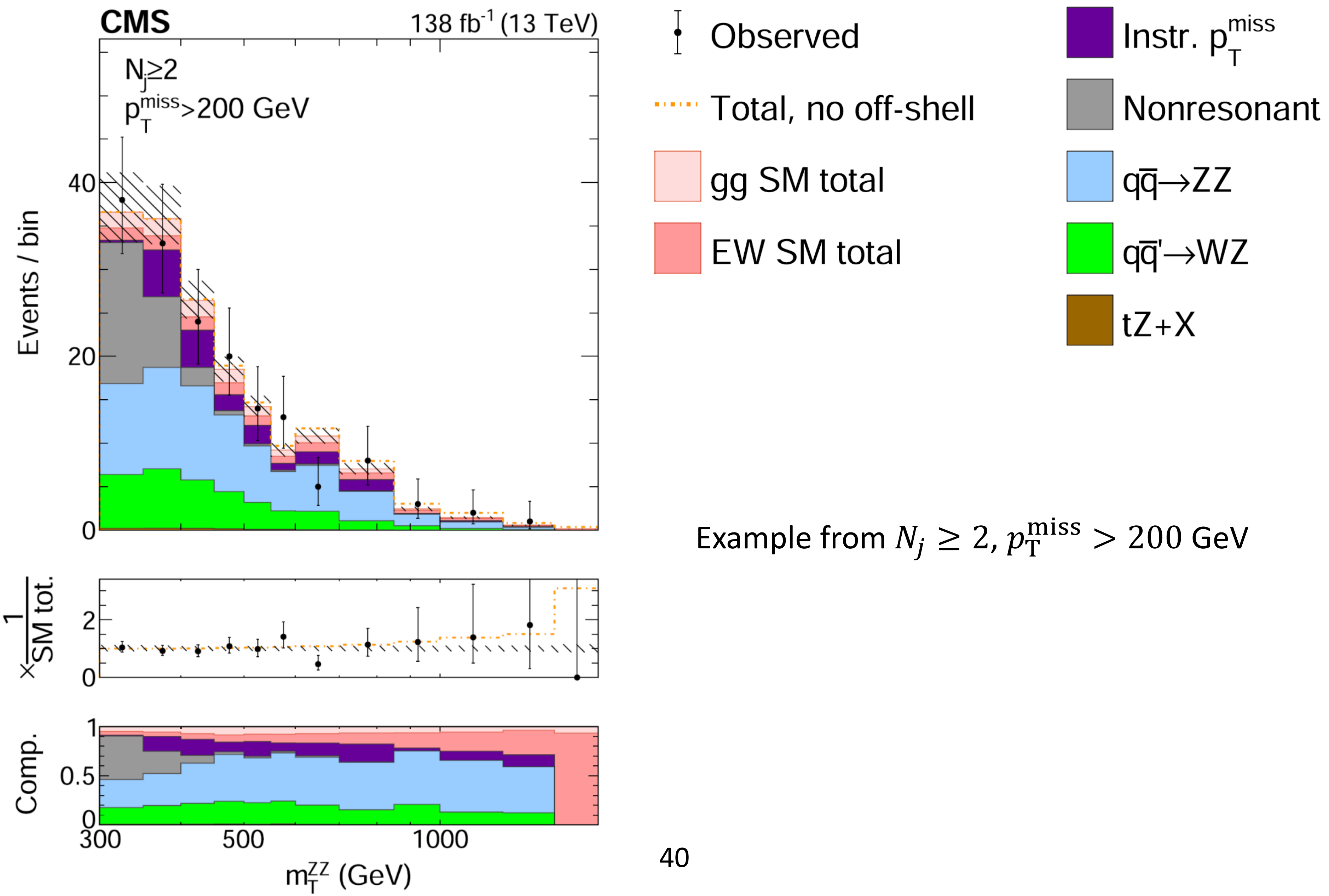

Example from $N_j \geq 2$, $p_T^{\text{miss}} > 200$ GeV

Off-shell $2\ell 2\nu$: Event distributions

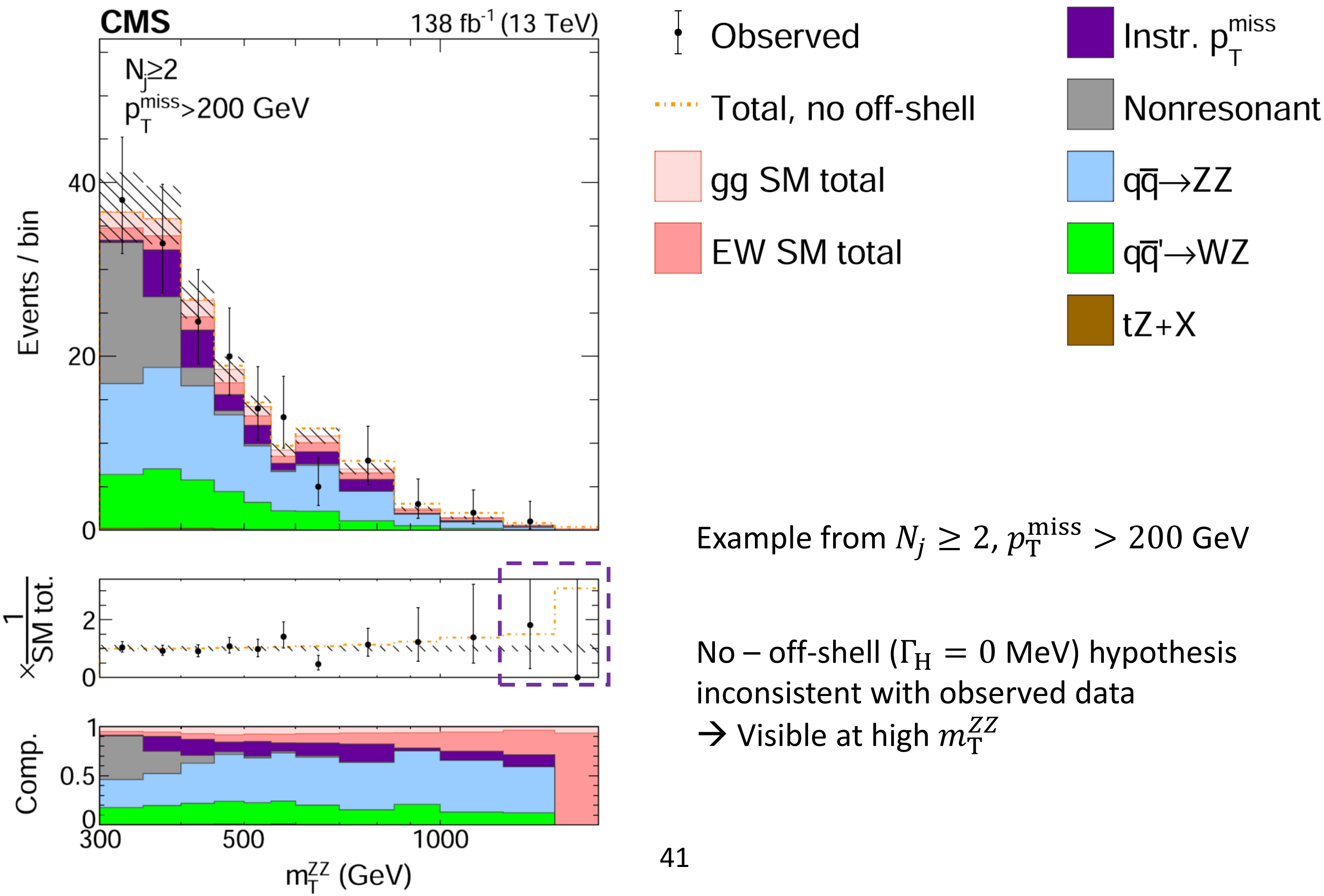

Example from $N_j \geq 2$, $p_{\mathrm{T}}^{\mathrm{miss}} > 200$ GeV

No – off-shell ($\Gamma_{\mathrm{H}} = 0$ MeV) hypothesis inconsistent with observed data
→ Visible at high m_{T}^{ZZ}

Off-shell $2\ell2\nu$: Golden VBF/VBS event

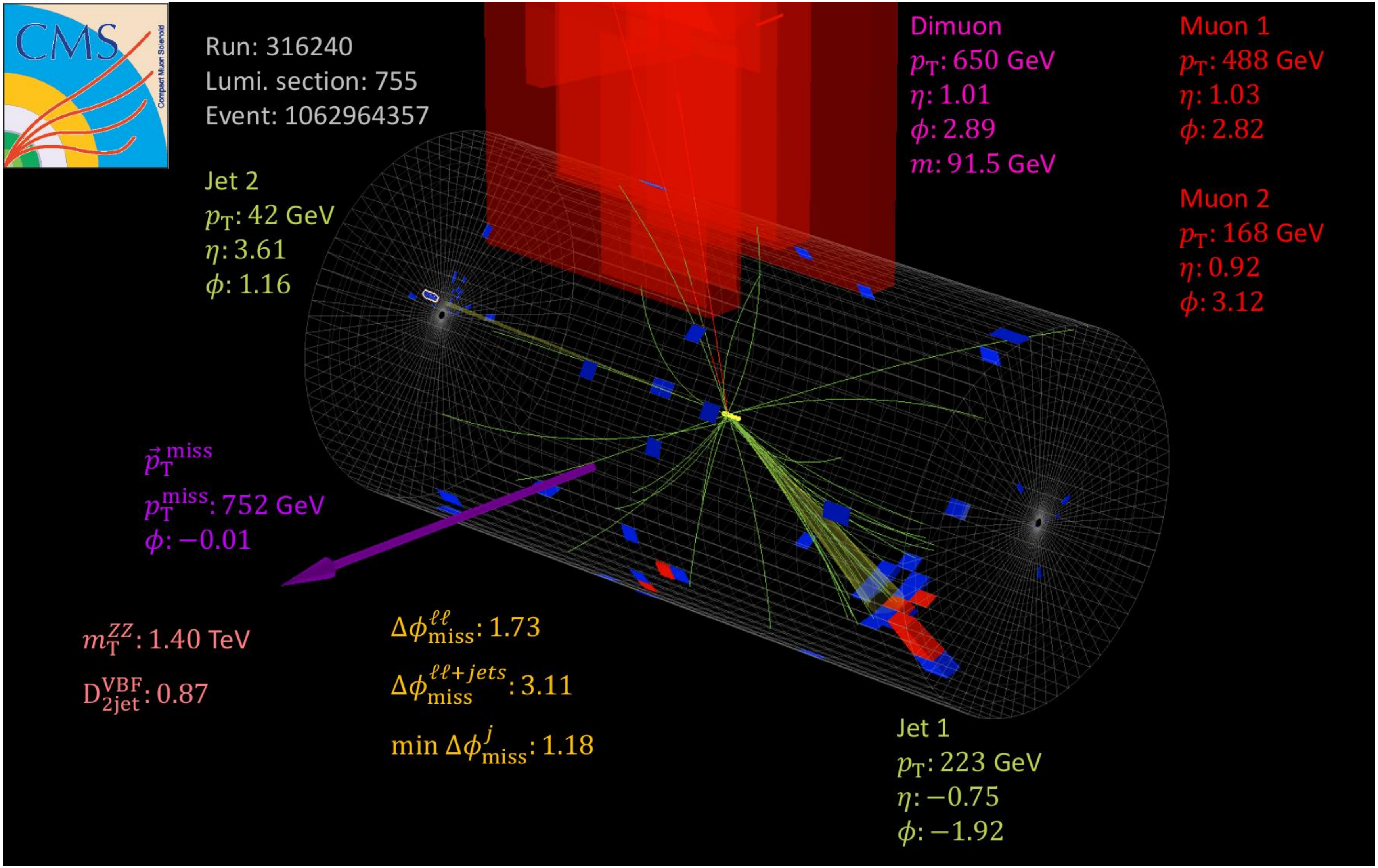

Here is a clean VBF/VBS $ZZ(\rightarrow 2\mu2\nu)$+2 jets candidate at high mass with large D_{2jet}^{VBF} value, as also evident from the two high-rapidity jets at opposite hemispheres.

Evidence for off-shell from $2\ell 2\nu + 4\ell$

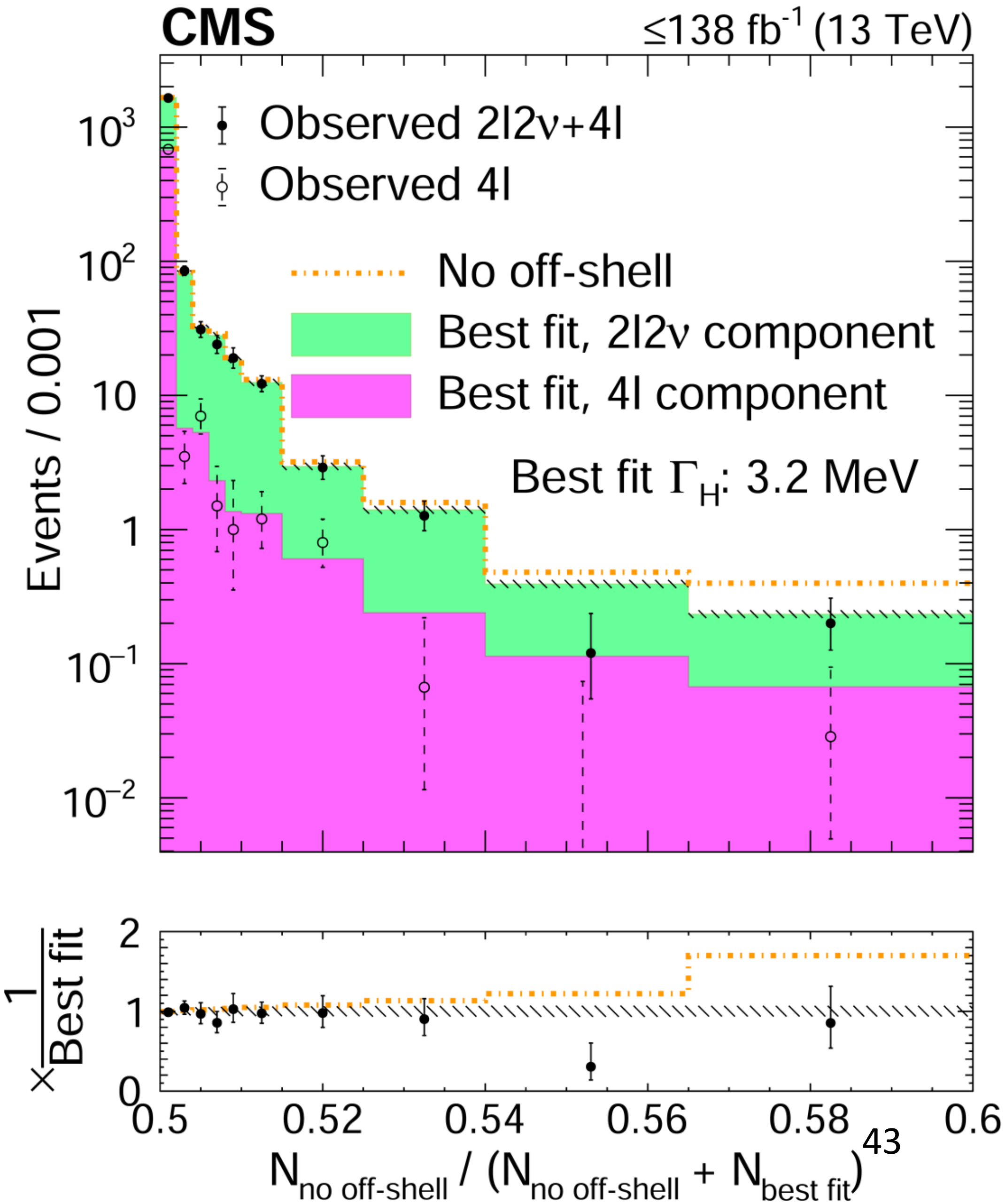

Plotted is a bin-by-bin ratio over the histograms of all observables and categories.

Evidence for off-shell from $2\ell 2\nu + 4\ell$

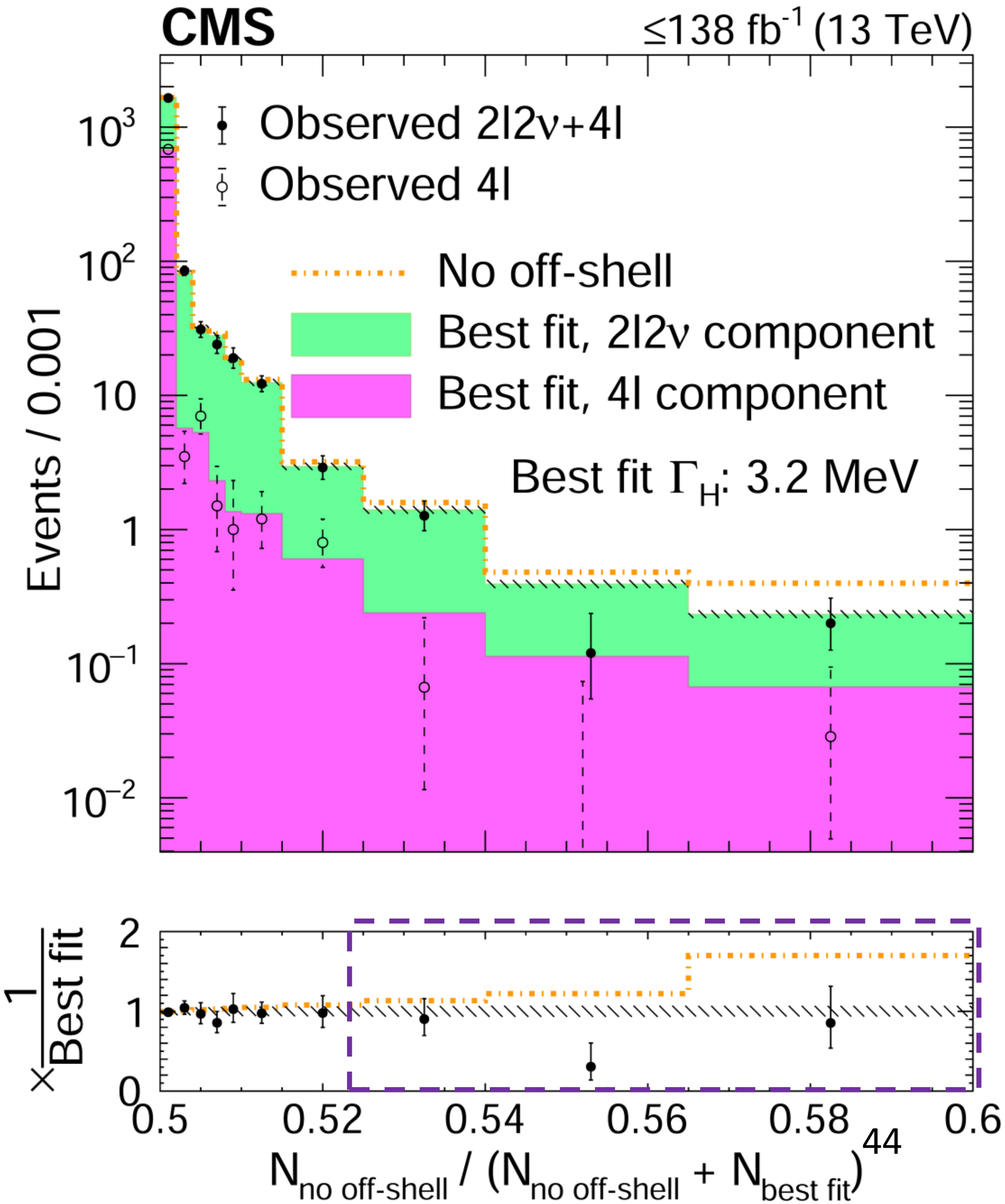

Plotted is a bin-by-bin ratio over the histograms of all observables and categories.

Once all bins and channels are considered, significance reaches 3.6 standard deviations.

Evidence for off-shell from $2\ell 2\nu + 4\ell$

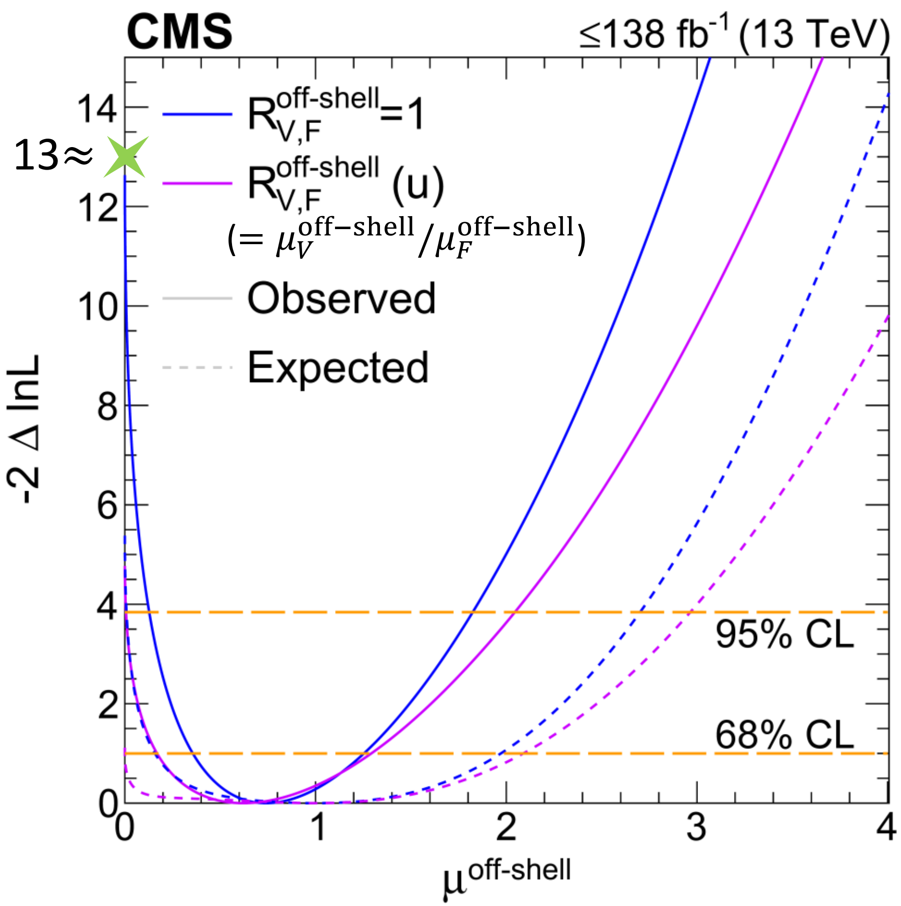

No – off-shell scenario ($\mu^{\text{off-shell}} = 0$) is excluded at p=0.0003 (3.6 std. devs.)

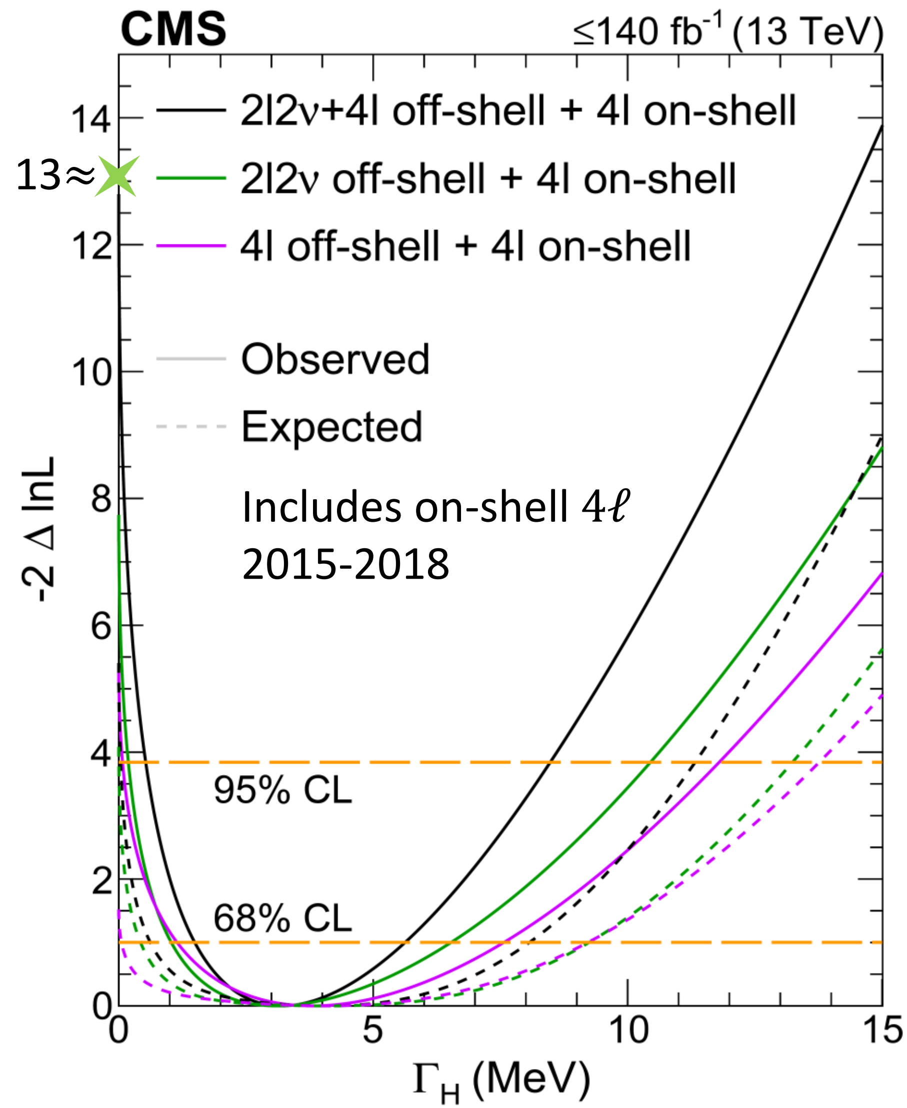

Observed $\Gamma_H = 3.2^{+2.4}_{-1.7}$ MeV
[0.5, 8.5] MeV @ 95% CL

Off-shell combination: $\mu_F^{\mathrm{off-shell}}, \mu_V^{\mathrm{off-shell}}$

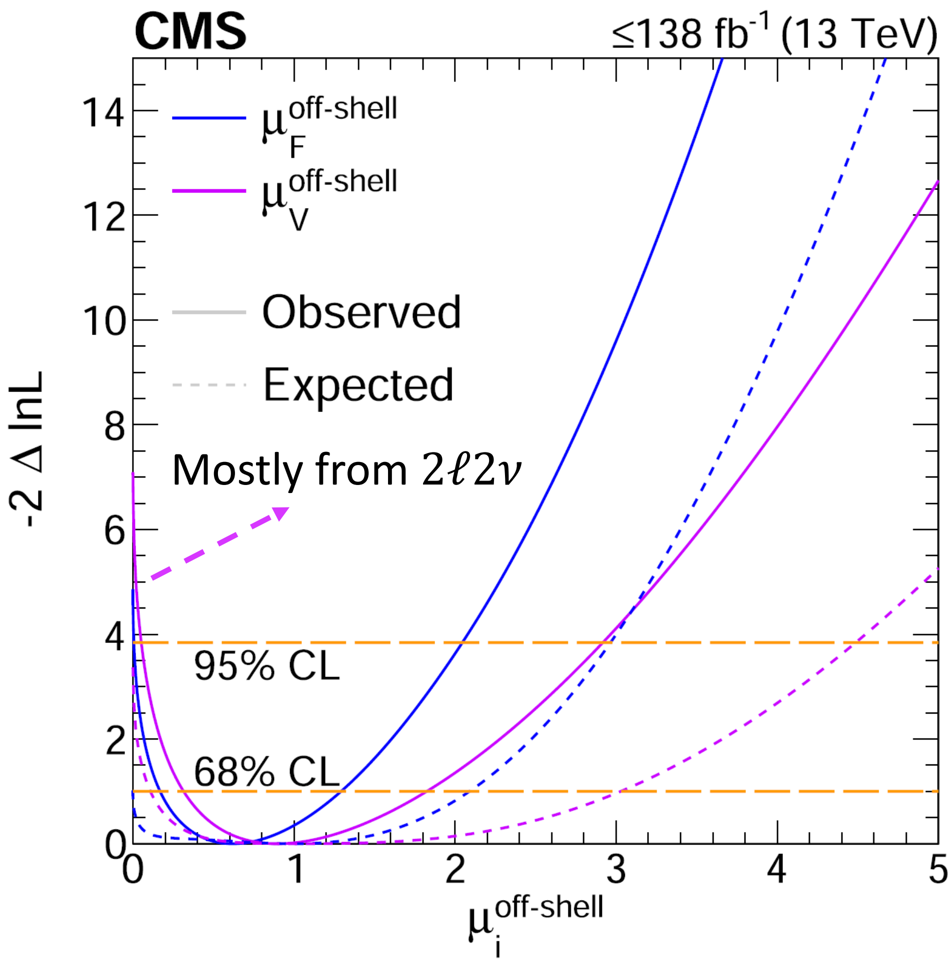

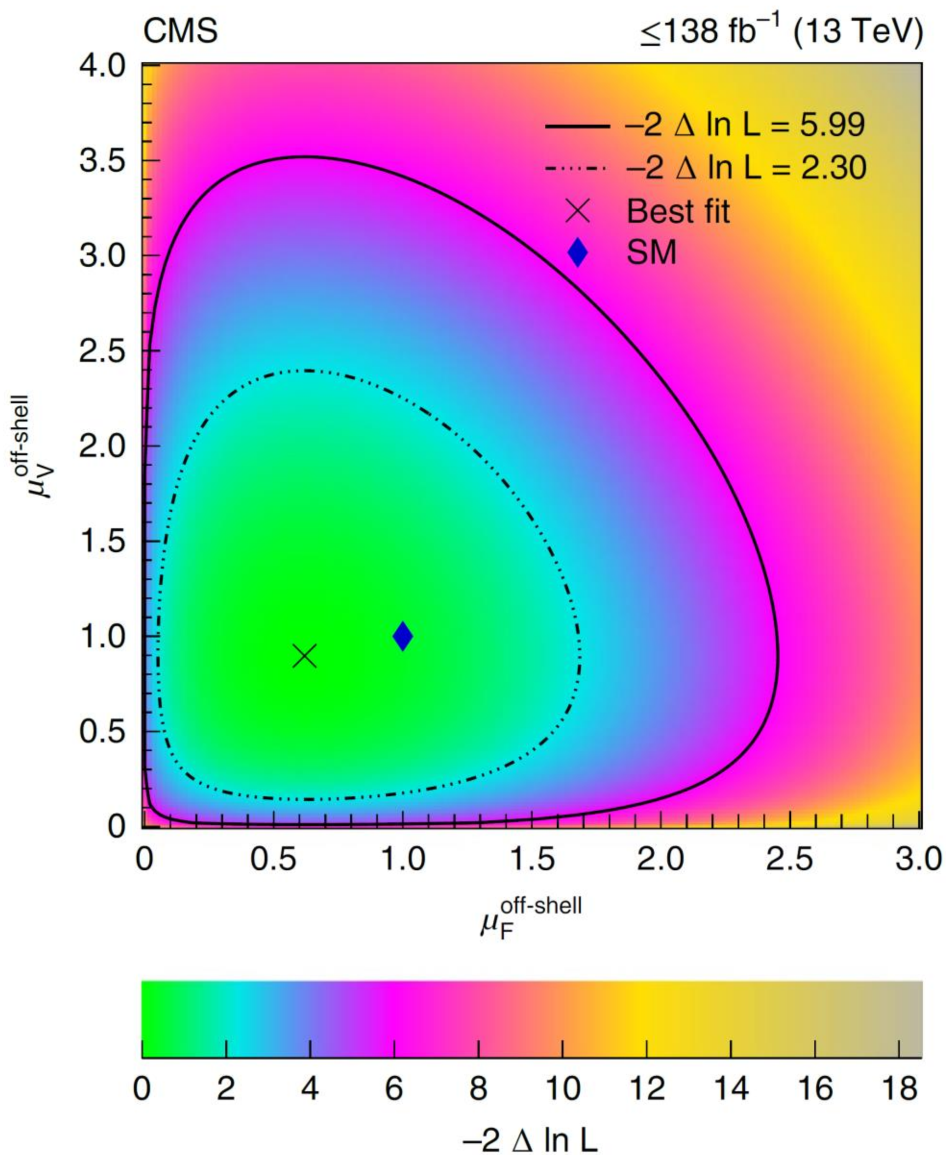

Joint constraints on
$\mu_F^{\mathrm{off-shell}}$ (gg production) and
$\mu_V^{\mathrm{off-shell}}$ (EW production)

Anomalous HVV couplings from off-shell

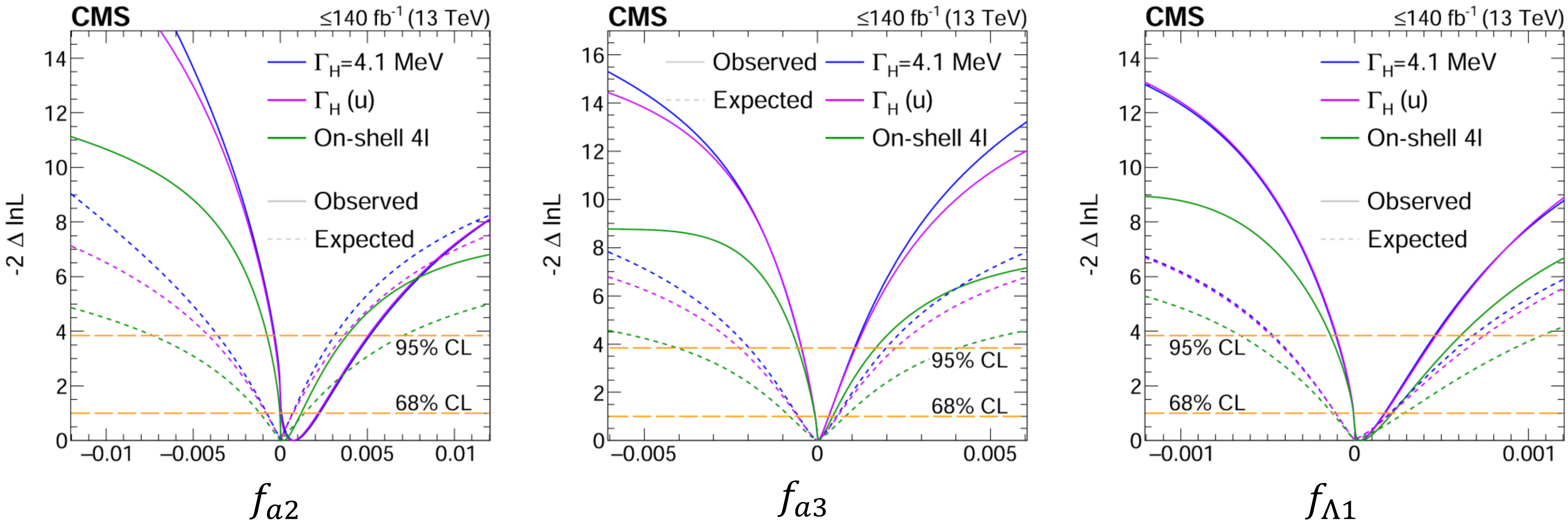

O$(10^{-5}$–$10^{-3})$ constraints on fractional BSM contributions

O(10%) improvement from adding off-shell information

Other on-shell - only measurements [1] are consistent with these results and the SM, and constrain these couplings even further.

Anomalous HVV couplings from off-shell

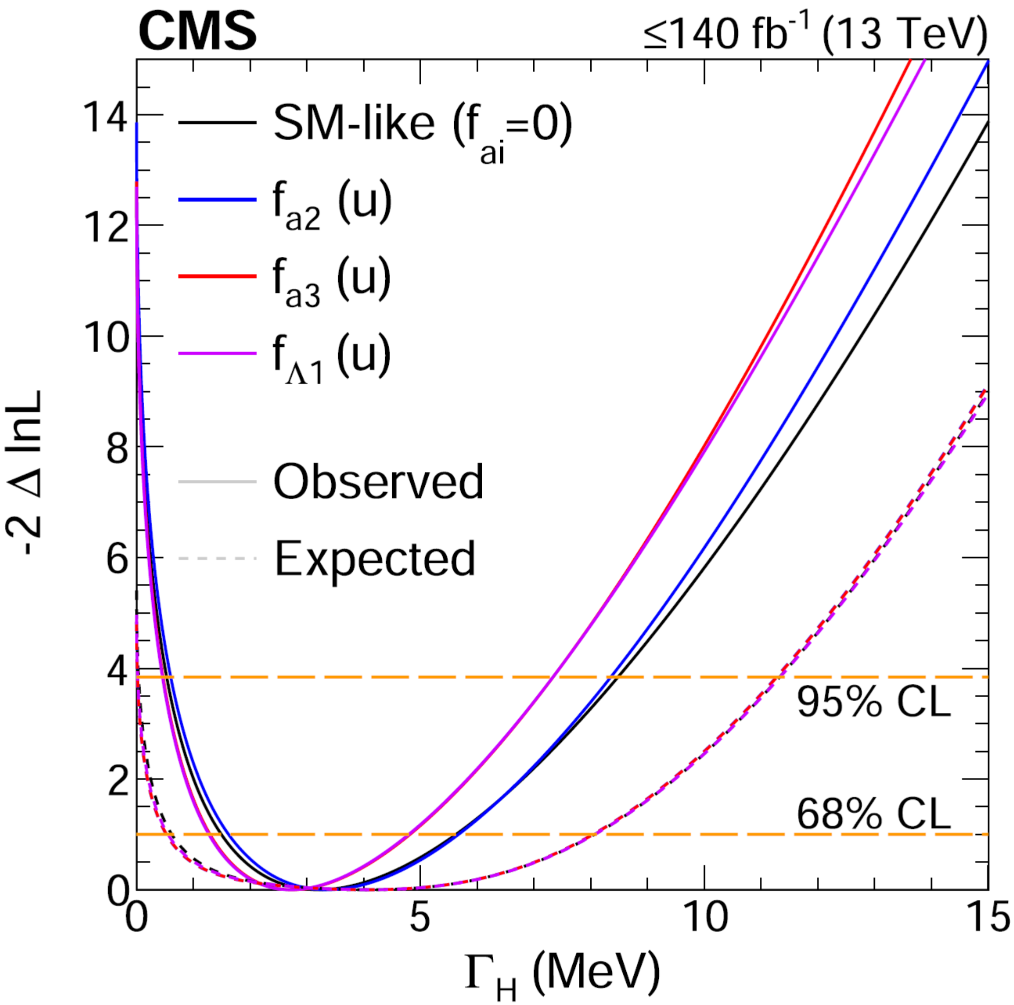

Measurement of the width is also stable when different anomalous HVV couplings are tested.

Summary

Presented the current status of the off-shell analysis:
→ Off-shell Higgs production in VV final states Important in the SM for unitarity
→ Combination with on-shell information can allow us to measure the total width
  → Large deviations can hint at BSM couplings to the Higgs boson

→ Analysis consists of 4ℓ off-shell and on-shell, and $2\ell 2\nu$ off-shell components
  → Particular emphasis is given today on the most recent $2\ell 2\nu$ off-shell analysis
  → Additional WZ CR promising to constraint the main non-interfering $q\bar{q} \to ZZ$ bkg.

→ Evidence for off-shell Higgs boson contributions in the $\mathrm{ZZ} \to 4\ell + 2\ell 2\nu$ final state

→ Best total width measurement from CMS is now $\Gamma_{\mathrm{H}} = 3.2^{+2.4}_{-1.7}$ MeV.
  → Measurement is stable if anomalous HVV couplings, which have the largest impact on kinematics, are considered.

Stay tuned for more exciting results as we continue to collect data in Run 3 and develop analysis methods further!

Back-up

Off-shell & BSM ggH couplings

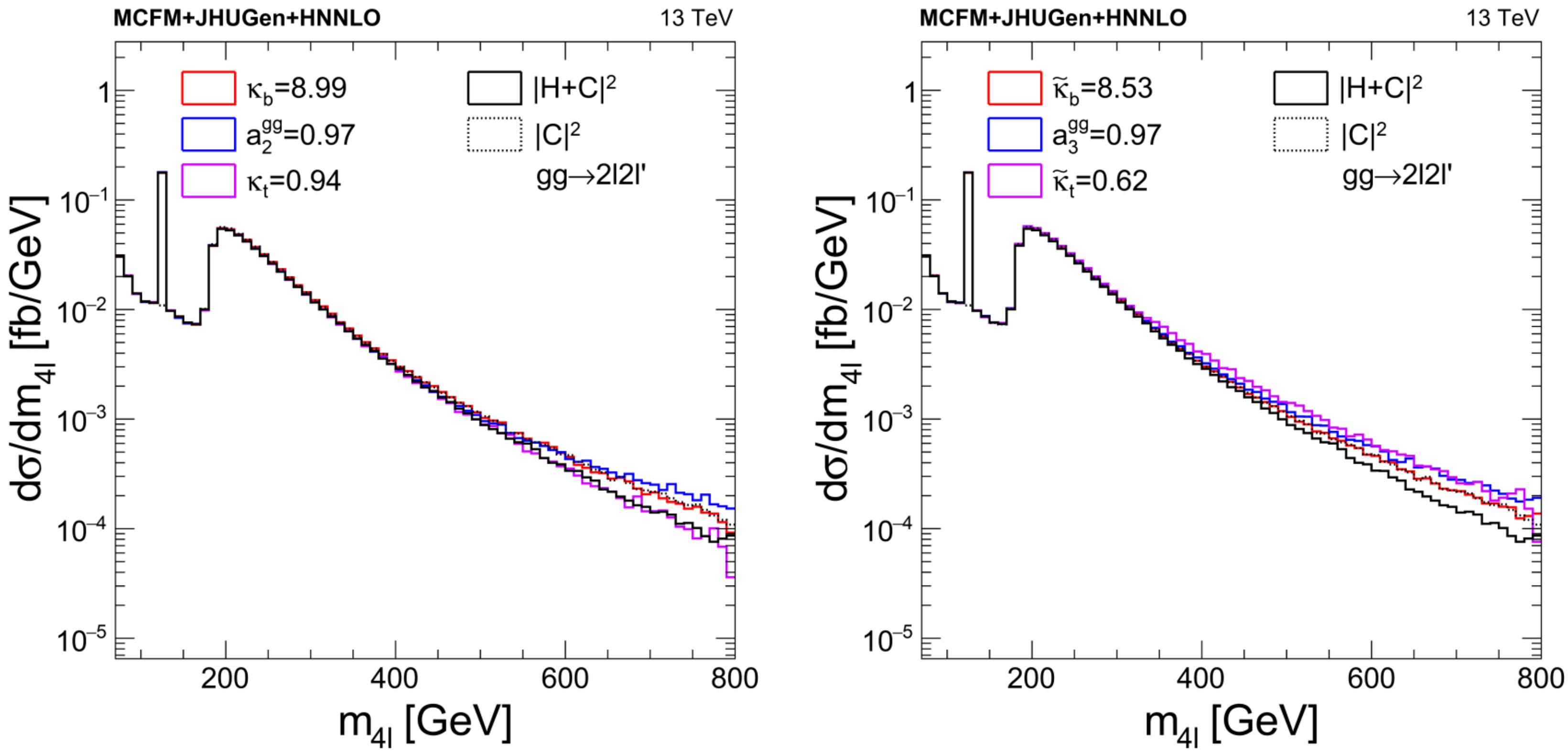

$$A(ggH) \sim \sum_f \kappa_f F_f(q_1, q_2 | m_f) + \tilde{\kappa}_f \tilde{F}_f(q_1, q_2 | m_f)$$
$$+ |a_2|\, e^{i\phi_{a2}}\, f^{*(1)}_{\mu\nu} f^{*(2),\mu\nu} + |a_3|\, e^{i\phi_{a3}}\, f^{*(1)}_{\mu\nu} \tilde{f}^{*(2),\mu\nu}$$

Effects [1] only visible for a *purely BSM Higgs boson* beyond ~500 GeV, couplings constrained to a fraction of these values [2]

Similar conclusions from couplings that affect the continuum [3,4]

No sensitivity with current number of events, so we assume gg couplings are as in the SM.

[1] Sarica, U. Springer Theses (2019)
[2] CMS Collaboration (2022); arxiv:2205.05120
[2] LHC Higgs Off-shell Subgroup; CDS:2801789 (2022)
[3] SMEFiT Collaboration; JHEP 11 089 (2021) (arxiv:2105.00006)

Gluon fusion: Higgs amplitude

$gg \to H \to ZZ$:

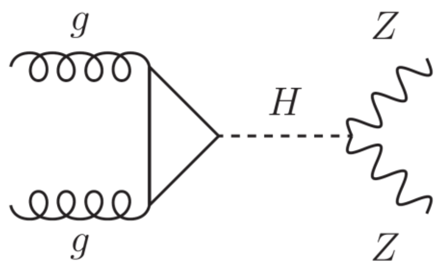

Full cross section calculation is available at different orders for the different components:
→ $gg \to H \to ZZ$: $\mathrm{N^3LO}$ in QCD around $m_H = 125$ GeV, NNLO for the full m_{ZZ} dependence, NLO or LO for event simulation [1]

→ K-factors are large for NLO/LO (~1.7-1.8), smaller and flatter for NNLO/NLO (~1.2-1.3), and the $\mathrm{N^3LO}$/NNLO K-factor is 1.10.

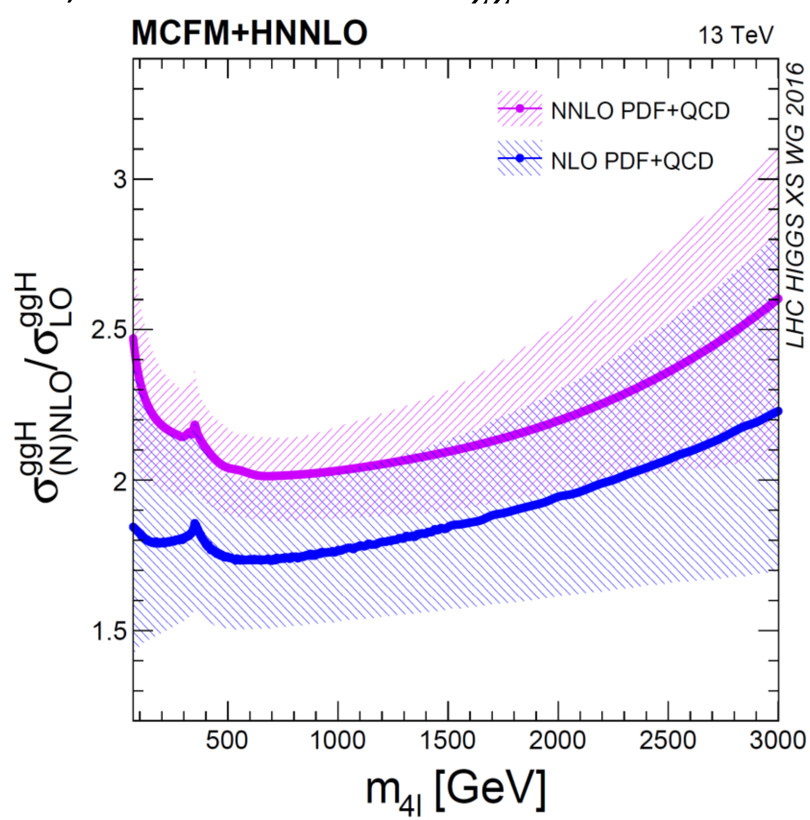

[1] LHC Higgs WG; CERN-2017-002-M (arxiv:1610.07922)

Gluon fusion: Continuum amplitude

$gg \to ZZ$:

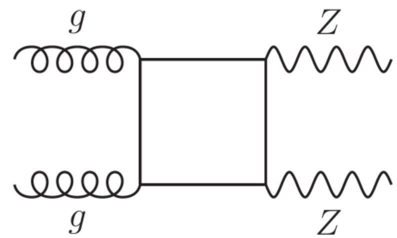

Full cross section calculation is available at different orders for the different components:
→ $gg \to ZZ$ continuum (and interference): Only full calculation and simulation with loop effects available at LO in QCD

- → Approximate NLO calculations [1] show K-factors for $gg \to ZZ$ continuum, $gg \to H \to ZZ$, and their interference within ~10% suggesting corrections are mostly of soft/collinear nature
- → Current procedure is to use K-factors for $gg \to H \to ZZ$ on all components, and unc. $\kappa_{ggZZ} = 1 \pm 0.1$ on continuum with related scale $\sqrt{\kappa_{ggZZ}}$ on interference.

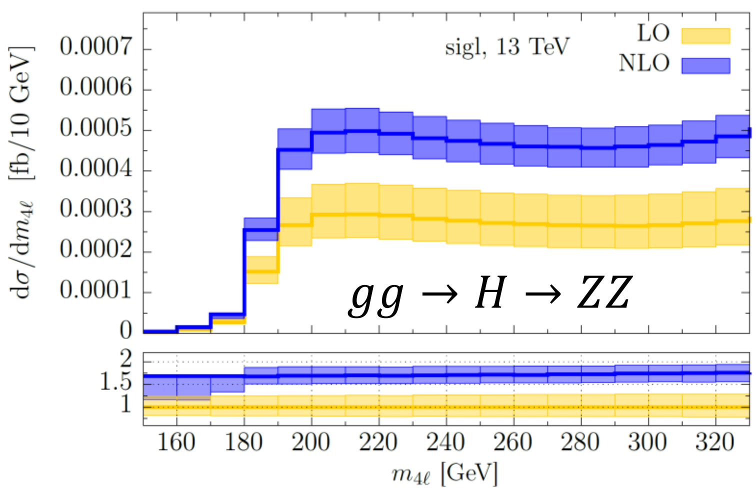

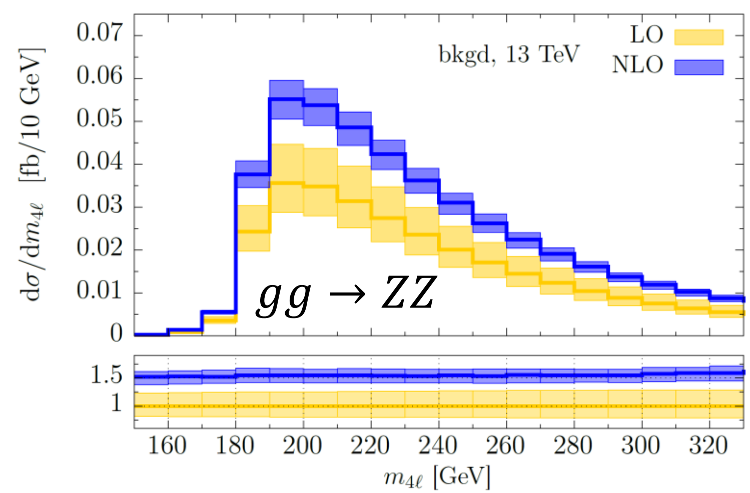

[1] Caola, F. et al.; JHEP 07 087 (2016) (arxiv:1605.04610)

Gluon fusion: Event generation

For the Higgs amplitude contribution, continuum ZZ, or interference, MC event generation can be done in two ways [1]:

→ Use JHUGen/MCFM to produce events at LO in QCD, apply NNLO K-factors and $\mathrm{N^3LO}$ flat normalization

→ Relies on Pythia for jet multiplicity and kinematics

→ Use POWHEG to produce $gg \to H$, JHUGen for $H \to ZZ$, and the MELA matrix elements from JHUGen/MCFM (instead of event generation) to obtain continuum ZZ and interference.

→ POWHEG cannot produce off-shell line shape. Instead, produce samples for Higgs samples at m_H =125, 160 ... 200 ... 3000 GeV, which have increasingly larger widths.

→ $\mathrm{hfact} = m_H/10 + 37.5$ GeV to match p_T^H to NNLO+NNLL HRES predictions.

→ For the $gg \to H(125) \to ZZ$ amplitude, the only differences in these samples are the propagator and the correction of the m_{ZZ} line shape for the evolution of BR($H \to ZZ$).

The former is just reweighting the propagator to a BW($m_H = 125$ GeV, $\Gamma_H = 4.1$ MeV), so it is basically part of the MELA reweighting procedure, and the latter is added as a modification of event weights when running the JHUGen decay step.

→ The samples are glued together in the end to produce the full spectrum. The mathematical formulation is provided extensively in the note.

→ We observe this approach produces stable results in jet multiplicity and other kinematics after Pythia parton shower.

[1] CMS Collaboration; CMS-NOTE-2022-010, CDS:2826782

Gluon fusion: Jet-exclusive

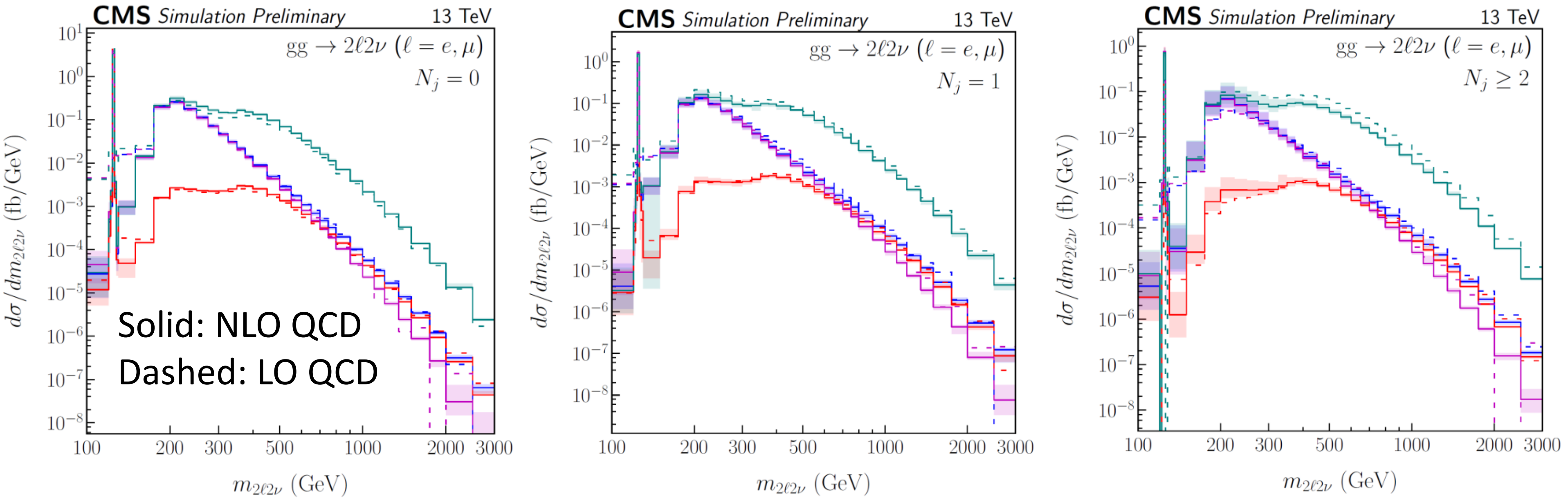

Analyses need better control over jet multiplicity and kinematics than what MC LO in QCD + parton shower can provide.

When split by jet (*) multiplicity, $N_j = 0{,}1$ have similar levels of agreement
→ LO m_{ZZ} distortion at $N_j \geq 2$ understood to be because of parton shower effects

(*) Gen.-level anti-k$_T$ $\Delta R = 0.4$ jets with $p_T > 30$ GeV, $|\eta| < 4.7$

[1] CMS Collaboration; CMS-NOTE-2022-010, CDS:2826782

EW production simulation

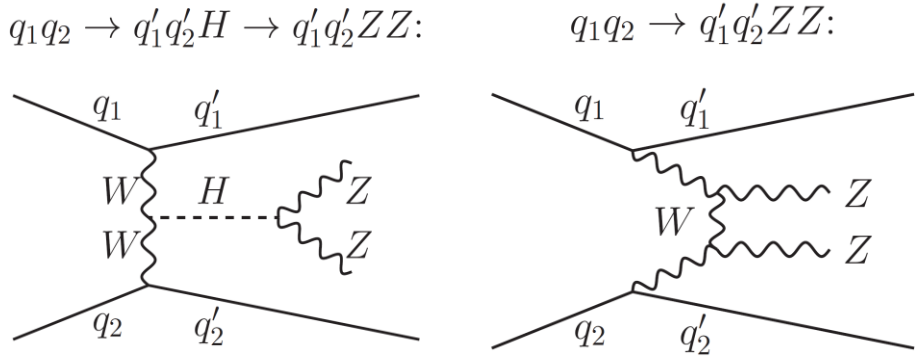

Matrix element (MELA) and event simulation (MCFM/JHUGen) available for SM or BSM Higgs hypotheses, and continuum at LO in QCD consistently.

→ Improve event simulation technique for jet kinematics [1] by

- starting with POWHEG+JHUGen samples for NLO VBF, and ZH and WH NLO + MiNLO HVJ)
- apply MELA ME reweighting

→ Account for the extra partons from POWHEG by merging four-momenta of gluons (or $g \to q\bar{q}$ decays) to the closest quark

→ We check that the LO topology is approximated decently.

[1] CMS Collaboration; CMS-NOTE-2022-010, CDS:2826782

EW process: Jet-exclusive distributions

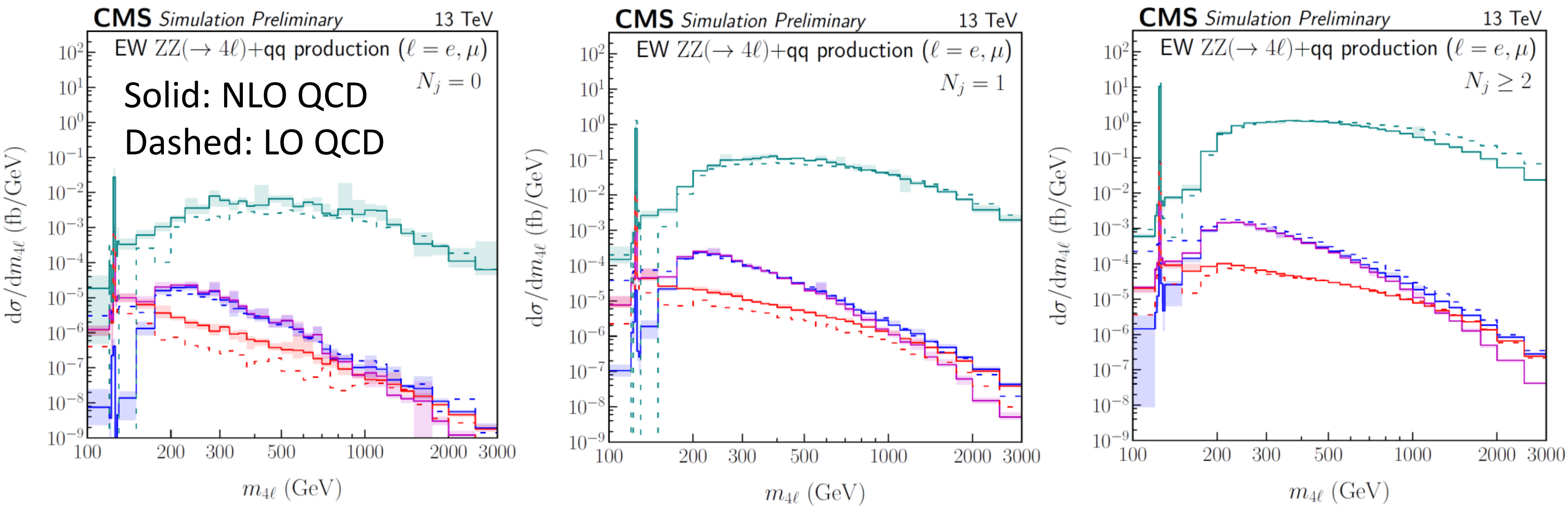

Analyses need better control over jet multiplicity and kinematics than what MC LO in QCD + parton shower can provide.

When events are split by jet multiplicity and equivalent selection requirements are placed on the LO and NLO MC, we find differences in $N_j = 0{,}1$.
→ Discrepancies are understood to be from imprecise parton shower modelling in the LO MC.

[1] CMS Collaboration; CMS-NOTE-2022-010, CDS:2826782

EW processes: Recasting NLO topology to LO

The MELA and MELAANALYTICS packages impose several rules on the merging procedure for the EW processes in order to make sensible predictions:

- An incoming gluon is never merged into an incoming quark. This rule is invoked implicitly as the q^2 of the incoming partons is always the largest compared to that of any other pair of partons in the event.
- Gluons are never merged into the decay products of the H boson from the JHUGen step as they are produced during the production of the H boson with no prior knowledge about the boson's decay.
- Gluons are also never merged into the decay products of the associated W or Z boson in the VH samples. Doing so distorts the BW nature of these resonances significantly.
- All merging is done in the convention of outgoing particles. This means the four-momenta and charge of incoming particles are reversed in the intermediate steps when those of the two merged particles are summed.
- When an incoming gluon is merged into an outgoing quark, the charge (i.e., PDG id) and the four-momentum of the quark are reversed in the final step of the LO topology construction. This reversion is done so that the event topology ensures having exactly two incoming quarks as expected in the LO matrix elements.
- In the VH samples, when extra gluons are encountered, the merging of individual gluons and that of a combined gluon (i.e., from a $g \to gg$ process) are all considered separately.
- In the VH samples, it is also possible to encounter two extra quarks instead of gluons. These extra quarks are merged into a gluon substitute first, as they are from a $g \to q\overline{q}$ branching process, before the merging of this gluon substitute is considered.
- Every merging permutation is considered, rated with the product of the dot-products between the merged quarks and gluons, and those that do not produce an incoming-outgoing parton composition that is compatible with the main physics process of the sample (i.e., VBF, ZH, or WH) are skipped.
- A momentum redistribution procedure is applied on the incoming and outgoing particles associated with H boson production so that the resultant topology features massless particles, which is what is required from the use of massless spinors in matrix elements. Denoting the momenta of the two final incoming or outgoing partons as p_1 and p_2, an intermediate four-momentum k is added to p_1 and subtracted from p_2 such that $|p_1 + k|^2 = |p_2 - k|^2 = 0$. This step is common to any matrix element computed using the MELA package. Because event-by-event reweighting is done through a ratio of matrix elements, which are invariant under any arbitrary boost of the event topology, and because factors coming from PDFs cancel in the ratio, the common boost of all particles does not affect reweighting as long as momentum conservation is maintained strictly, and is therefore adjusted arbitrarily.

[1] CMS Collaboration; CMS-NOTE-2022-010, CDS:2826782

$q\bar{q} \rightarrow ZZ, WZ$ simulation

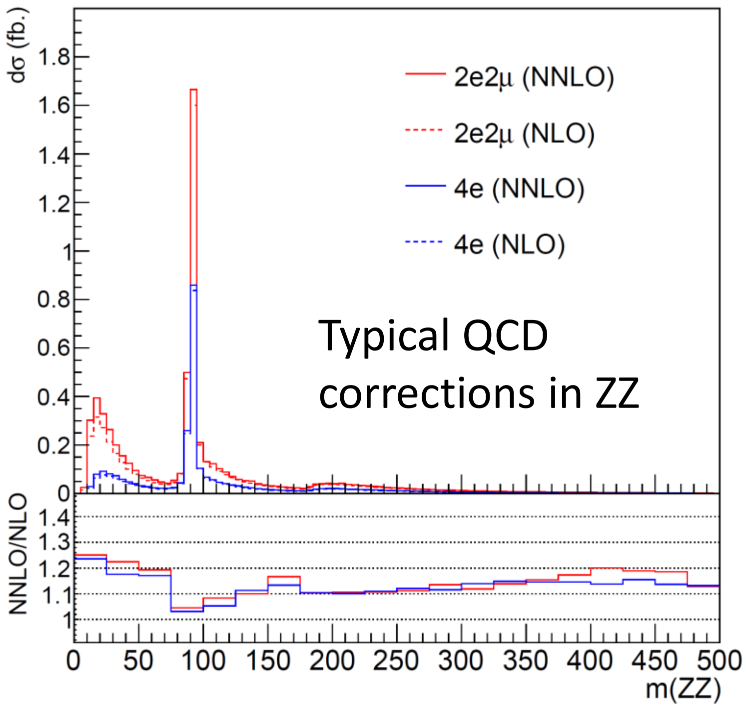

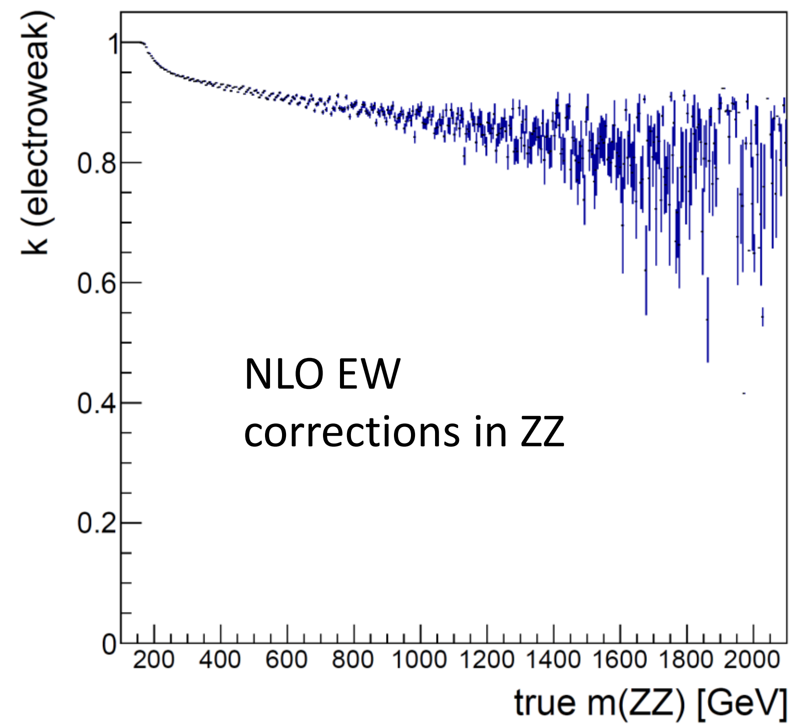

POWHEG simulation at NLO in QCD is used for the non-interfering ZZ and WZ backgrounds.
→ NNLO QCD corrections can be calculated as a function of m_{ZZ}.
→ Relative uncertainties from the MC close to NNLO QCD cross section uncertainties
→ Keep the relative uncs. as in the MC to predict the uncertainty in different kinematic regions and jet categories

$q\bar{q} \rightarrow ZZ, WZ$ simulation

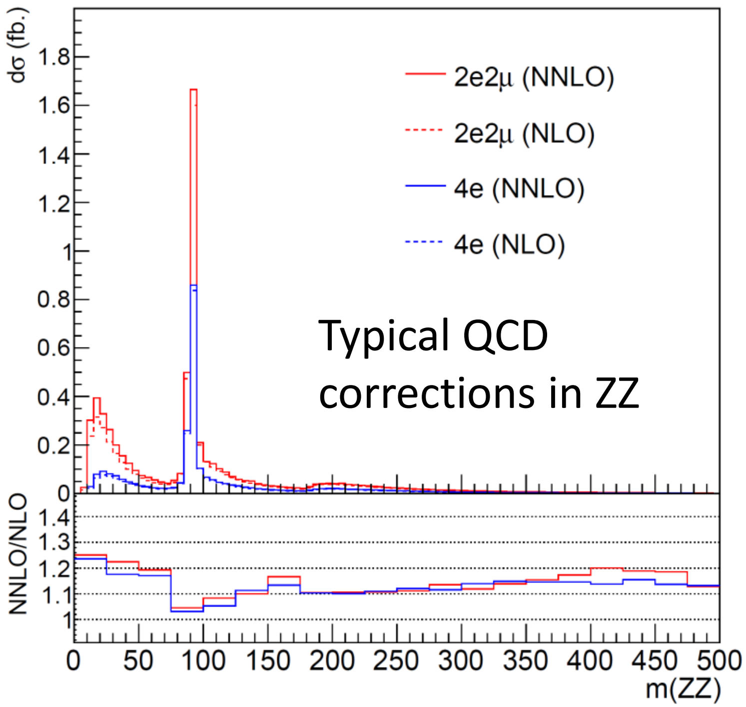

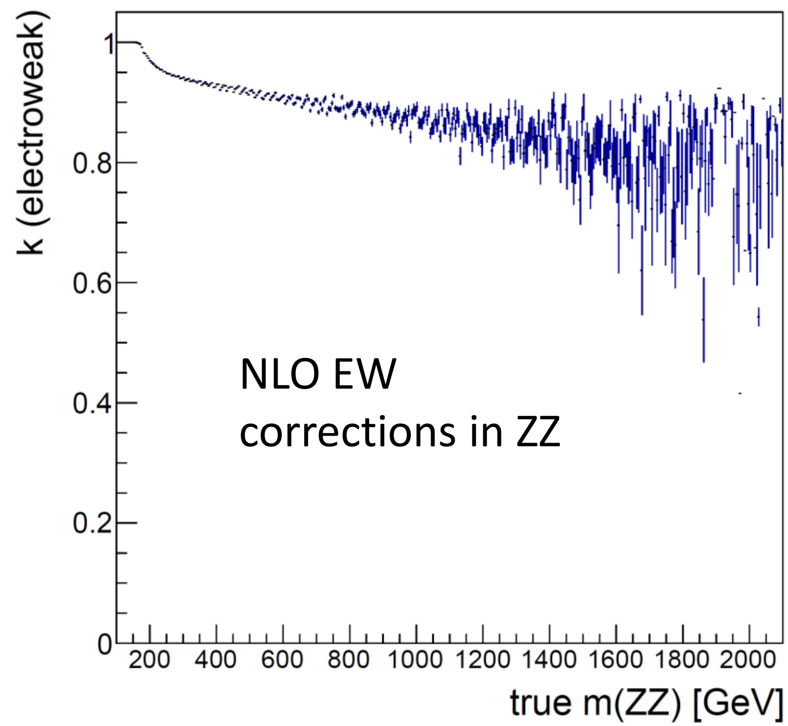

POWHEG simulation at NLO in QCD is used for the non-interfering ZZ and WZ backgrounds.

→ NLO EW corrections typically reach -20% in ZZ (-10% in WZ) at ~1 TeV [1].

→ Assign the following uncertainty prescription [2] based on $\rho = \frac{\left|\sum_i \vec{p}_{\mathrm{T}}^{\,i}\right|}{\sum_i \left|\vec{p}_{\mathrm{T}}^{\,i}\right|}$ over leptons:

$$\delta = \begin{cases} \left(1 - K_{QCD}^{NLO}\right)\left(1 - K_{EW}^{NLO}\right) & \text{if } \rho < 0.3 \\ \left(1 - K_{EW}^{NLO}\right) & \text{otherwise} \end{cases}$$

[1] Bierweiler, A. et al.; JHEP 12 071 (2013) (arxiv:1305.5402)
[2] Gieseke, S. et al.; EPJ C 74 2988 (2014) (arxiv:1401.3964)

Full table of observables for off-shell 4ℓ

Category	VBF-tagged	VH-tagged	Untagged
Selection	$\mathcal{D}_{\rm 2jet}^{\rm VBF}$ or $\mathcal{D}_{\rm 2jet}^{\rm VBF,BSM} > 0.5$	$\mathcal{D}_{\rm 2jet}^{\rm WH}$ or $\mathcal{D}_{\rm 2jet}^{\rm WH,BSM}$, or $\mathcal{D}_{\rm 2jet}^{\rm ZH}$ or $\mathcal{D}_{\rm 2jet}^{\rm ZH,BSM} > 0.5$	Rest of events
SM obs.	$m_{4\ell}, \mathcal{D}_{\rm bkg}^{\rm VBF+dec}, \mathcal{D}_{\rm bsi}^{\rm VBF+dec}$	$m_{4\ell}, \mathcal{D}_{\rm bkg}^{\rm VH+dec}, \mathcal{D}_{\rm bsi}^{\rm VH+dec}$	$m_{4\ell}, \mathcal{D}_{\rm bkg}^{\rm kin}, \mathcal{D}_{\rm bsi}^{\rm gg,dec}$
a_3 obs.	$m_{4\ell}, \mathcal{D}_{\rm bkg}^{\rm VBF+dec}, \mathcal{D}_{0-}^{\rm VBF+dec}$	$m_{4\ell}, \mathcal{D}_{\rm bkg}^{\rm VH+dec}, \mathcal{D}_{0-}^{\rm VH+dec}$	$m_{4\ell}, \mathcal{D}_{\rm bkg}^{\rm kin}, \mathcal{D}_{0-}^{\rm dec}$
a_2 obs.	$m_{4\ell}, \mathcal{D}_{\rm bkg}^{\rm VBF+dec}, \mathcal{D}_{0h+}^{\rm VBF+dec}$	$m_{4\ell}, \mathcal{D}_{\rm bkg}^{\rm VH+dec}, \mathcal{D}_{0h+}^{\rm VH+dec}$	$m_{4\ell}, \mathcal{D}_{\rm bkg}^{\rm kin}, \mathcal{D}_{0h+}^{\rm dec}$
Λ_1 obs.	$m_{4\ell}, \mathcal{D}_{\rm bkg}^{\rm VBF+dec}, \mathcal{D}_{\Lambda 1}^{\rm VBF+dec}$	$m_{4\ell}, \mathcal{D}_{\rm bkg}^{\rm VH+dec}, \mathcal{D}_{\Lambda 1}^{\rm VH+dec}$	$m_{4\ell}, \mathcal{D}_{\rm bkg}^{\rm kin}, \mathcal{D}_{\Lambda 1}^{\rm dec}$

Full table of observables for on-shell 4ℓ

2016-2018 categorization follows the order
- VBF-2 jet
- VH-hadronic
- VH-leptonic (1 lepton or an $\ell^+\ell^-$ pair)
- VBF-1 jet
- Boosted
- Untagged

Category	Selection	Observables $\vec{x}$ for fitting
Boosted	$p_T^{4\ell} > 120\,\text{GeV}$	$\mathcal{D}_{\text{bkg}}, p_T^{4\ell}$
VBF-1jet	$\mathcal{D}_{\text{1jet}}^{\text{VBF}} > 0.7$	$\mathcal{D}_{\text{bkg}}, p_T^{4\ell}$
VBF-2jet	$\mathcal{D}_{\text{2jet}}^{\text{VBF}} > 0.5$	$\mathcal{D}_{\text{bkg}}^{\text{EW}}, \mathcal{D}_{0h+}^{\text{VBF+dec}}, \mathcal{D}_{0-}^{\text{VBF+dec}}, \mathcal{D}_{\Lambda 1}^{\text{VBF+dec}}, \mathcal{D}_{\Lambda 1}^{Z\gamma,\text{VBF+dec}}, \mathcal{D}_{\text{int}}^{\text{VBF}}, \mathcal{D}_{CP}^{\text{VBF}}$
VH-hadronic	$\mathcal{D}_{\text{2jet}}^{\text{VH}} > 0.5$	$\mathcal{D}_{\text{bkg}}^{\text{EW}}, \mathcal{D}_{0h+}^{\text{VH+dec}}, \mathcal{D}_{0-}^{\text{VH+dec}}, \mathcal{D}_{\Lambda 1}^{\text{VH+dec}}, \mathcal{D}_{\Lambda 1}^{Z\gamma,\text{VH+dec}}, \mathcal{D}_{\text{int}}^{\text{VH}}, \mathcal{D}_{CP}^{\text{VH}}$
VH-leptonic	see Section 3	$\mathcal{D}_{\text{bkg}}, p_T^{4\ell}$
Untagged	none of the above	$\mathcal{D}_{\text{bkg}}, \mathcal{D}_{0h+}^{\text{dec}}, \mathcal{D}_{0-}^{\text{dec}}, \mathcal{D}_{\Lambda 1}^{\text{dec}}, \mathcal{D}_{\Lambda 1}^{Z\gamma,\text{dec}}, \mathcal{D}_{\text{int}}^{\text{dec}}, \mathcal{D}_{CP}^{\text{dec}}$

Off-shell $2\ell 2\nu$: Event selection

Quantity	Requirement
p_{T}^{ℓ}	$p_{\mathrm{T}}^{\ell} \geq 25\,\mathrm{GeV}$ on both leptons
$\lvert\eta_{\ell}\rvert$	< 2.4 on μ, < 2.5 on e
$m_{\ell\ell}$	$\lvert m_{\ell\ell} - 91.2\rvert < 15\,\mathrm{GeV}$
$p_{\mathrm{T}}^{\ell\ell}$	$\geq 55\,\mathrm{GeV}$
N_{ℓ}	Exactly two leptons with tight isolation, no extra leptons with loose isolation and $p_{\mathrm{T}} \geq 5\,\mathrm{GeV}$
N_{trk}	No isolated tracks satisfying the selection requirements
N_{γ}	No photons with $p_{\mathrm{T}} \geq 20\,\mathrm{GeV}$, $\lvert\eta\rvert < 2.5$ satisfying the baseline selection requirements
p_{T}^{j}	$\geq 30\,\mathrm{GeV}$, used in selecting jets
$\lvert\eta_{j}\rvert$	< 4.7, used in selecting jets
N_{b}	No b-tagged jets based on the loose working point
$p_{\mathrm{T}}^{\mathrm{miss}}$	$\geq 125\,\mathrm{GeV}$ if $N_j < 2$, $\geq 140\,\mathrm{GeV}$ otherwise
$\Delta\phi_{\mathrm{miss}}^{\ell\ell}$	> 1.0 between $\vec{p}_{\mathrm{T}}^{\,\ell\ell}$ and $\vec{p}_{\mathrm{T}}^{\,\mathrm{miss}}$
$\Delta\phi_{\mathrm{miss}}^{\ell\ell+\mathrm{jets}}$	> 2.5 between $\vec{p}_{\mathrm{T}}^{\,\ell\ell} + \sum \vec{p}_{\mathrm{T}}^{\,\mathrm{j}}$ and $\vec{p}_{\mathrm{T}}^{\,\mathrm{miss}}$
$\min \Delta\phi_{\mathrm{miss}}^{\mathrm{j}}$	> 0.25 if $N_j = 1$, > 0.5 otherwise among all $\vec{p}_{\mathrm{T}}^{\,\mathrm{j}}$ and $\vec{p}_{\mathrm{T}}^{\,\mathrm{miss}}$ combinations

Requirements are mainly aimed toward reducing
- instrumental $p_{\mathrm{T}}^{\mathrm{miss}}$ smearing from Z+jets
- $t\bar{t} \rightarrow 2\ell 2\nu 2b$
- WW $\rightarrow 2\ell 2\nu$

Off-shell $2\ell 2\nu$: $q\bar{q} \rightarrow ZZ, WZ$

Quantity	Requirement
$p_T^{\ell_{Z1}}$	$\geq 30\,\text{GeV}$ on leading-p_T lepton forming the Z candidate
$p_T^{\ell_{Z2}}$	$\geq 20\,\text{GeV}$ on subleading-p_T lepton forming the Z candidate
$p_T^{\ell_W}$	$\geq 20\,\text{GeV}$ on the remaining ℓ_W from the W boson
$\lvert\eta_\ell\rvert$	< 2.4 on μ, < 2.5 on e
$m_{\ell\ell}$	Use the opposite-sign, same-flavor dilepton pair with smallest $\lvert m_{\ell\ell} - 91.2\rvert < 15\,\text{GeV}$ to define the Z candidate
N_ℓ	Exactly three leptons with tight isolation, no extra leptons with loose isolation and $p_T \geq 5\,\text{GeV}$
N_{trk}	No isolated tracks satisfying the selection requirements
N_γ	No photons with $p_T \geq 20\,\text{GeV}$, $\lvert\eta\rvert < 2.5$ satisfying the baseline selection requirements
p_T^j	$\geq 30\,\text{GeV}$, used in selecting jets
$\lvert\eta_j\rvert$	< 4.7, used in selecting jets
N_b	No b-tagged jets based on the loose working point
p_T^{miss}	$\geq 20\,\text{GeV}$
$m_T^{\ell_W}$	$\geq 20\,\text{GeV}$ ($10\,\text{GeV}$) for $\ell_W = \mu$ ($\ell_W = \text{e}$), where $m_T^{\ell_W} = \sqrt{2 p_T^{\ell_W} p_T^{\text{miss}} \left(1 - \cos\Delta\phi_{\text{miss}}^{\ell_W}\right)}$ is the transverse mass between $\vec{p}_T^{\,\ell_W}$ and $\vec{p}_T^{\text{ miss}}$
$A \times m_T^{\ell_W} + p_T^{\text{miss}} \geq 120\,\text{GeV}$, with $A = 1.6\ (4/3)$ for $\ell_W = \mu$ (e)	
$\Delta\phi_{\text{miss}}^{Z}$	> 1.0 between $\vec{p}_T^{\,Z}$ and $\vec{p}_T^{\text{ miss}}$
$\Delta\phi_{\text{miss}}^{3\ell+\text{jets}}$	> 2.5 between $\vec{p}_T^{\,3\ell} + \sum \vec{p}_T^{\,j}$ and $\vec{p}_T^{\text{ miss}}$
$\min \Delta\phi_{\text{miss}}^{j}$	> 0.25 among all $\vec{p}_T^{\,j}$ and $\vec{p}_T^{\text{ miss}}$ combinations

Estimated using POWHEG simulation at NLO in QCD
→ Additional K-factors for NLO EW and NNLO QCD corrections are applied.
→ A joint fit with a 3ℓ WZ CR is done with common nuisance parameters and m_T^{WZ} as the only observable:

$$m_T^{WZ^2} = \left[\sqrt{p_T^{\ell\ell^2} + m_{\ell\ell}^2} + \sqrt{\left|\vec{p}_T^{\text{ miss}} + \vec{p}_T^{\,\ell_W}\right|^2 + m_W^2}\right]^2 - \left|\vec{p}_T^{\,\ell\ell} + \vec{p}_T^{\,\ell_W}\right|^2$$

→ Events in the CR are categorized for the same N_j bins, and $\ell_W = e, \mu$.